

# Analyzing Error Sources in Global Feature Effect Estimation

Timo Heiß<sup>1,2</sup>[0009-0002-0392-4308], Coco Bögel<sup>1,2</sup>[0009-0002-0683-4957], Bernd Bischl<sup>1,2</sup>[0000-0001-6002-6980], and Giuseppe Casalicchio<sup>1,2</sup>[0000-0001-5324-5966]

<sup>1</sup> LMU Munich, Munich, Germany

{timo.heiss,giuseppe.casalicchio}@stat.uni-muenchen.de

<sup>2</sup> Munich Center for Machine Learning (MCML)

**Abstract.** Global feature effects such as partial dependence (PD) and accumulated local effects (ALE) plots are widely used to interpret black-box models. However, they are only estimates of true underlying effects, and their reliability depends on multiple sources of error. Despite the popularity of global feature effects, these error sources are largely unexplored. In particular, the practically relevant question of whether to use training or holdout data to estimate feature effects remains unanswered. We address this gap by providing a systematic, estimator-level analysis that disentangles sources of bias and variance for PD and ALE. To this end, we derive a mean-squared-error decomposition that separates model bias, estimation bias, model variance, and estimation variance, and analyze their dependence on model characteristics, data selection, and sample size. We validate our theoretical findings through an extensive simulation study across multiple data-generating processes, learners, estimation strategies (training data, validation data, and cross-validation), and sample sizes. Our results reveal that, while using holdout data is theoretically the cleanest, potential biases arising from the training data are empirically negligible and dominated by the impact of the usually higher sample size. The estimation variance depends on both the presence of interactions and the sample size, with ALE being particularly sensitive to the latter. Cross-validation-based estimation is a promising approach that reduces the model variance component, particularly for overfitting models. Our analysis provides a principled explanation of the sources of error in feature effect estimates and offers concrete guidance on choosing estimation strategies when interpreting machine learning models.

**Keywords:** Interpretable Machine Learning · Feature Effects · Partial Dependence Plot · Accumulated Local Effects

## 1 Introduction

Many machine learning models are black boxes whose internal structure is not, or only partly, compatible with human reasoning, complicating explanations of both individual predictions and overall model behavior. This lack of transparency is especially problematic in high-stakes domains such as healthcare, law, and

finance, where decisions must be transparent. To address this challenge, the field of eXplainable AI (XAI) has proposed a wide range of methods to explain machine learning models [16]. However, these methods must be used correctly to avoid misleading conclusions, as there are many pitfalls to be aware of [18].

Global feature effect methods such as partial dependence (PD) [7] and accumulated local effects (ALE) [1] visualize how one or more features affect predictions. In practice, they are estimated from finite data, and their reliability depends on various error sources. Despite their widespread adoption, the error components of feature effect estimates remain largely unexplored. Prior works focus on extrapolation under feature dependence [1,9], aggregation bias [9,10,12,13], or quantifying uncertainty [1,5,19]. A formal bias–variance decomposition w.r.t. a true underlying effect has only been derived for the theoretical PD [17], leaving estimator-level errors introduced by finite data largely unaddressed.

A related practical question is whether to estimate explanations using training or holdout data. This has been studied for methods like permutation feature importance (PFI) [18], mean decrease in impurity (MDI), and SHAP [14], but remains open for PD and ALE. While most works compute feature effects on training data [1,7,11,16], other works use holdout data [17]. Practitioners still debate whether to estimate PD and ALE on training or holdout data (see §2), trading larger training sample sizes against potential overfitting bias. These open questions point to a lack of an estimator-level understanding of error in global feature effect estimation, which our work addresses. Our main contributions are:

- We provide the first estimator-level analysis of PD and ALE, deriving a full mean squared error (MSE) decomposition that separates model bias, estimation bias, model variance, and estimation variance.
- We theoretically analyze these components, showing how sample size and interactions affect estimation bias and variance differently for PD and ALE, and formally relating remaining bias and variance to model bias and variance.
- We empirically validate our findings in an extensive simulation study across multiple data-generating processes, learners, sample sizes, and estimation strategies (training, validation, and cross-validation (CV)), using dedicated estimators for the error components. We find negligible bias differences between training and holdout data, a strong sample-size effect – especially for ALE – and that CV is often preferable due to variance reduction.

## 2 Related Work

Many issues in feature effects have been analyzed. The PD plot [7] is known to suffer from extrapolation under dependent features by evaluating the model on implausible feature combinations [18]. ALE plots avoid exactly that issue [1]. Another issue is *aggregation bias*: global effects can obscure interaction-induced heterogeneity. Individual conditional expectation (ICE) curves [10] and RHALE [9] visualize this heterogeneity, while regional methods like REPID [12] and GADGET [13] report effects in regions with reduced heterogeneity. Several works quantify uncertainty via variance of feature effects with model-specific PD confidence bands existing for probabilistic models [19], as well as model-agnostic

approaches that consider PD or ALE across multiple model fits [5,17,1]. Only a few works explicitly study bias–variance trade-offs in feature effect estimators. RHALE [9] optimizes ALE binning to balance bias and variance but does not relate this trade-off to a ground-truth effect. In [8], bias and variance of the proposed DALE estimator w.r.t. ALE are analyzed. In [3], variance reduction and consistency of their proposed ALE estimator A2D2E are shown, and the error of PD, ALE, and A2D2E estimators against a derivative-based ground-truth are compared in simulations. Moreover, [17] formalize PD as a statistical estimator of a target estimand, derive a formal MSE decomposition for the theoretical PD, and propose variance estimators for confidence intervals. In contrast, we provide the first full estimator-level MSE decomposition of empirical PD and ALE w.r.t. their corresponding ground-truth feature effects, and analyze the error and its components both theoretically and empirically.

For many interpretability methods, computing explanations on training vs. holdout data can affect conclusions: it matters for loss-based methods like permutation feature importance (PFI) [18] and for mean decrease in impurity (MDI) and SHAP, which can be biased on training data [14]. For feature effects, this issue is largely unstudied. PD [7], ALE [1], and common references and software often use training data without justification [11,16], while others use holdout data [17]. Practitioners likewise disagree: some prefer training data for more reliable estimates due to larger sample size<sup>3</sup>, others prefer holdout data as “the model may overfit”<sup>4</sup>, and some use both to diagnose distribution differences.<sup>5</sup> To date, no systematic study addresses this. We do so by comparing different estimation strategies (training/holdout/CV) through bias-variance decomposition.

### 3 Notation & Background

Assume a data-generating process that is characterized by a joint distribution  $\mathbb{P}_{XY}$  over features  $X = (X_1, \dots, X_p)^\top$  and target  $Y$ , with true underlying function  $f(x) = \mathbb{E}[Y \mid X = x]$ . A random dataset  $D = \{(X^{(i)}, Y^{(i)})\}_{i=1}^n$  consists of  $n$  i.i.d. samples from  $\mathbb{P}_{XY}$ . Concrete realizations  $\mathcal{D} = \{(\mathbf{x}^{(i)}, y^{(i)})\}_{i=1}^n$  are the training, test, and validation sets  $\mathcal{D}_{\text{train}}$ ,  $\mathcal{D}_{\text{test}}$ , and  $\mathcal{D}_{\text{val}}$ . A learning algorithm induces a fitted model  $\hat{f}$  on  $\mathcal{D}_{\text{train}}$ , viewed either as a fixed function or as a random variable with distribution  $\mathbb{P}_F$  due to training-sample and algorithmic randomness. Model performance is measured by the risk  $R_L(\hat{f}) = \mathbb{E}_{XY}[L(Y, \hat{f}(X))]$  with a point-wise loss  $L$ , and can be estimated on an  $n$ -sized dataset  $\mathcal{D}$  as empirical risk  $R_{\text{emp}}(\hat{f}; \mathcal{D}) = \frac{1}{n} \sum_{i=1}^n L(y^{(i)}, \hat{f}(\mathbf{x}^{(i)}))$ . For  $\mathcal{D}_{\text{train}}$ , this measures in-sample, for  $\mathcal{D}_{\text{test}}$  or  $\mathcal{D}_{\text{val}}$  out-of-sample error. Expectations and variances w.r.t.  $\hat{f} \sim \mathbb{P}_F$  are denoted by subscript  $F$ ,  $D \sim \mathbb{P}_{XY}$  by  $D$ , and  $(X, Y) \sim \mathbb{P}_{XY}$  by  $XY$  (analogously for marginal and conditionals). Note that  $D$  and  $\hat{f}$  are independent (denoted  $D \perp \hat{f}$ ) only if  $D$  is not used for training, i.e., only for holdout data.

<sup>3</sup> <https://forums.fast.ai/t/partial-dependence-plot/98465> (last accessed: 01/28/2026)

<sup>4</sup> <https://github.com/sosuneko/PDPbox/issues/68> (01/28/2026)

<sup>5</sup> <https://www.mathworks.com/help/stats/use-partial-dependence-plots-to-interpret-regression-models-trained-in-regression-learner-app.html> (01/28/2026)

We consider feature effects for a subset of features  $X_S$  with  $S \subseteq \{1, \dots, p\}$ . Throughout this work, we restrict attention to a single feature of interest ( $|S| = 1$ ) and denote the complement feature set by  $X_{\bar{S}}$ .

**Definition 1 (PD [7]).** Let  $h : \mathcal{X} \rightarrow \mathcal{Y}$  be a prediction function and let  $X_S$  denote a feature of interest. The PD of  $h$  w.r.t.  $X_S$  is defined as

$$PD_{h,S}(x_S) := \mathbb{E}_{X_{\bar{S}}}[h(x_S, X_{\bar{S}})] = \int_{\mathcal{X}_{\bar{S}}} h(x_S, \mathbf{x}_{\bar{S}}) d\mathbb{P}_{X_{\bar{S}}}(\mathbf{x}_{\bar{S}}). \quad (1)$$

Given an  $n$ -sized dataset  $\mathcal{D}$ , it can be estimated via Monte Carlo integration as  $\widehat{PD}_{h,S}(x_S) := \frac{1}{n} \sum_{i=1}^n h(x_S, \mathbf{x}_{\bar{S}}^{(i)}) = \frac{1}{n} \sum_{i=1}^n h_S^{(i)}(x_S)$ .

Here,  $h_S^{(i)}(x_S) = h(x_S, \mathbf{x}_{\bar{S}}^{(i)})$  are the ICE curves [10].  $PD_{\hat{f},S}$  denotes the theoretical PD of the model  $\hat{f}$ , and  $\widehat{PD}_{\hat{f},S}$  is its estimator.  $PD_{f,S}$  is the ground-truth PD. In practice, PD is visualized using a grid of  $G$  feature values  $\{x_S^{(g)}\}_{g=1}^G$ . Quantile-based grids rather than equidistant ones are recommended in [18].

**Definition 2 (ALE [1]).** Let  $h : \mathcal{X} \rightarrow \mathcal{Y}$  be a prediction function and let  $X_S$  denote a feature of interest. The uncentered ALE of  $h$  w.r.t.  $X_S$  is defined as

$$\widetilde{ALE}_{h,S}(x_S) = \lim_{K \rightarrow \infty} \sum_{k=1}^{k_S^K(x_S)} \mathbb{E}_{X_{\bar{S}} | X_S \in I_S^K(k)} [\Delta_{h,S}^K(k, X_{\bar{S}})], \quad (2)$$

where feature  $X_S$  is partitioned into  $K$  intervals  $\{I_S^K(k) = (z_{k-1,S}^K, z_{k,S}^K]\}_{k=1}^K$ ,  $k_S^K(x_S)$  denotes the index of the interval into which a value  $x_S$  falls, and the maximum interval width converges to zero as  $K \rightarrow \infty$ . The finite differences in the  $k$ -th interval are given by  $\Delta_{h,S}^K(k, \mathbf{x}_{\bar{S}}) := h(z_{k,S}^K, \mathbf{x}_{\bar{S}}) - h(z_{k-1,S}^K, \mathbf{x}_{\bar{S}})$ .

The uncentered ALE for a finite dataset  $\mathcal{D}$  and finite  $K$  can be estimated as follows, where  $n_S^K(k)$  denotes the number of observations in the  $k$ -th interval:

$$\widetilde{ALE}_{h,S}(x_S) = \sum_{k=1}^{k_S^K(x_S)} \frac{1}{n_S^K(k)} \sum_{i: x_S^{(i)} \in I_S^K(k)} [\Delta_{h,S}^K(k, \mathbf{x}_{\bar{S}}^{(i)})].$$

Centered versions  $ALE_{h,S}$  and  $\widehat{ALE}_{h,S}$  are obtained by subtracting a constant such that they have zero mean w.r.t. the marginal distribution of  $X_S$  or the empirical distribution of  $\{x_S^{(i)}\}_{i=1}^n$ , respectively. For the grid  $\{z_{k,S}^K\}_{k=0}^K$ , empirical quantiles of  $\{x_S^{(i)}\}_{i=1}^n$  are recommended [1]. For readability, we omit the superscript  $K$  when  $K$  is fixed, and suppress the subscript  $S$  for PD and ALE.

In [17], it is shown that the MSE of the theoretical PD of  $\hat{f}$  w.r.t. to the theoretical ground-truth PD can be decomposed into squared bias and variance:

$$\mathbb{E}_F[(PD_f(x_S) - PD_{\hat{f}}(x_S))^2] = (PD_f(x_S) - \mathbb{E}_F[PD_{\hat{f}}(x_S)])^2 + \text{Var}_F[PD_{\hat{f}}(x_S)]. \quad (3)$$

The bias term relates to systematic model bias, and the variance term captures variability across model fits. For the empirical estimator  $\widehat{PD}_{\hat{f}}$ , Molnar et al. [17] further argue that Monte Carlo integration introduces an additional source of variance. Moreover, when estimated on holdout data,  $\widehat{PD}_{\hat{f}}$  is unbiased w.r.t.  $PD_{\hat{f}}$ , and unbiasedness of the model implies unbiasedness of the PD.<sup>6</sup>

<sup>6</sup> Proofs can be found in Appendices C & D of the arXiv version of [17].

While an analogous decomposition for ALE is not available, consistency results for the ALE estimator exist in [1]. To this end, they define a population version of the binned uncentered ALE for a prediction function  $h$  as  $\widetilde{ALE}_h^K(x_S) := \sum_{k=1}^{k_S(x_S)} \mathbb{E}_{X_{\bar{S}} | X_S \in I_S(k)}[\Delta_h(k, X_{\bar{S}})]$ . For the same  $K$  fixed bins,  $\widetilde{ALE}_h$  on an i.i.d.  $D \sim \mathbb{P}_{XY}$  converges to  $\widetilde{ALE}_h^K$  pointwise as  $n \rightarrow \infty$  almost surely, under mild integrability conditions. Moreover,  $\widetilde{ALE}_h^K$  converges pointwise to  $\widetilde{ALE}_h$  as the bin resolution  $K \rightarrow \infty$ . Thus,  $\widetilde{ALE}_h$  is jointly consistent for  $\widetilde{ALE}_h$  if  $n$  grows sufficiently fast relative to  $K$ .<sup>7</sup>

## 4 Theoretical Considerations & Estimators

For our theoretical analysis, we adopt several assumptions listed in §A.1.

### 4.1 Full Error Decomposition of the PD Estimator

Previous work [17] considers only the error decomposition of  $PD_{\hat{f}}$ . Since  $PD_{\hat{f}}$  cannot be determined when  $\mathbb{P}_{X_{\bar{S}}}$  is unknown and is estimated via Monte Carlo integration, we instead study the estimator's error. While [17] notes that this adds a variance term, we formally derive the MSE decomposition at fixed  $x_S$ , integrating over both  $\hat{f} \sim \mathbb{P}_F$  and the dataset  $D \sim \mathbb{P}_{XY}$  used for PD estimation:

$$\begin{aligned} \mathbb{E}_F \mathbb{E}_{D|\hat{f}} [(PD_f(x_S) - \widehat{PD}_{\hat{f}}(x_S))^2] &= (PD_f(x_S) - \mathbb{E}_F \mathbb{E}_{D|\hat{f}}[\widehat{PD}_{\hat{f}}(x_S)])^2 \\ &+ \text{Var}_F \mathbb{E}_{D|\hat{f}}[\widehat{PD}_{\hat{f}}(x_S)] + \mathbb{E}_F \text{Var}_{D|\hat{f}}[\widehat{PD}_{\hat{f}}(x_S)]. \end{aligned} \quad (4)$$

The proof is given in §A.2. The decomposition has three distinct terms, which we will analyze in more detail below: the squared bias and two variances.

**Bias.** The bias of the PD estimator (cf. first term in Eq. (4)) decomposes as:

$$\begin{aligned} \mathbb{E}_F \mathbb{E}_{D|\hat{f}}[\widehat{PD}_{\hat{f}}(x_S)] - PD_f(x_S) &= \\ \mathbb{E}_F[\mathbb{E}_{D|\hat{f}}[\widehat{PD}_{\hat{f}}(x_S)] - PD_{\hat{f}}(x_S)] + (\mathbb{E}_F[PD_{\hat{f}}(x_S)] - PD_f(x_S)) \end{aligned} \quad (5)$$

by adding and subtracting  $\mathbb{E}_F[PD_{\hat{f},S}(x_S)]$ . The first part vanishes by the unbiasedness of the PD estimator w.r.t. the theoretical model PD [17], if only the data used for Monte Carlo integration in the PD estimation is independent of the model  $\hat{f}$ . This is true for holdout data, but not necessarily for training data. For the second part, exchanging expectations (Fubini) yields (proof in §A.3):

$$\mathbb{E}_F[PD_{\hat{f}}(x_S)] - PD_f(x_S) = \mathbb{E}_{X_{\bar{S}}} \left[ \mathbb{E}_F[\hat{f}(x_S, X_{\bar{S}})] - f(x_S, X_{\bar{S}}) \right]. \quad (6)$$

Consequently, the term reduces to the model's bias averaged over  $\mathbb{P}_{X_{\bar{S}}}$ . Thus, for estimation on holdout data, the PD estimator's bias reduces to the average model bias, whereas estimation on training data may introduce additional bias.

<sup>7</sup> These consistency results can be found in Theorem 3 of the arXiv version of [1].

**Model variance.** The second term in Eq. (4) reflects the variance of the PD estimator w.r.t. the model distribution  $\mathbb{P}_F$ . When the PD is estimated on holdout data, it reduces to  $\text{Var}_F[\mathbb{E}_{D|\hat{f}}[\widehat{PD}_{\hat{f}}(x_S)]] = \text{Var}_F[PD_{\hat{f}}(x_S)]$  by the unbiasedness of the PD estimator w.r.t. the theoretical model PD. This is exactly the variance of the theoretical PD in Eq. (3). By exchanging expectations (Fubini/Tonelli) and applying Jensen’s inequality, we obtain an upper bound (proof in §A.4):

$$\text{Var}_F[PD_{\hat{f}}(x_S)] \leq \mathbb{E}_{X_S} \text{Var}_F[\hat{f}(x_S, X_S)]. \quad (7)$$

Thus, the theoretical PD variance at  $x_S$  is controlled by the average (pointwise) model variance w.r.t. the marginal distribution of  $X_S$ .

**Estimation variance.** The third term in Eq. (4) captures the variance w.r.t. the samples used to estimate the PD via Monte Carlo integration, which equals:

$$\mathbb{E}_F \text{Var}_{D|\hat{f}}[\widehat{PD}_{\hat{f}}(x_S)] = \frac{1}{n} \mathbb{E}_F \text{Var}_{D|\hat{f}}[\hat{f}(x_S, X_S)] \quad (8)$$

for any  $X_S \sim D|\hat{f}$ . The proof is given in §A.5. Consequently, the pointwise estimation variance of the PD depends on the sample size  $n$  and decreases at the rate  $\mathcal{O}(1/n)$ . It also depends on the expected variance of the ICE curves at  $x_S$ . Centering the PD via  $\widehat{PD}_{\hat{f}}(x_S) - \mathbb{E}_{D|\hat{f}}[\widehat{PD}_{\hat{f}}(X_S)]$  yields the variance of the centered ICE curves  $\text{Var}_{D|\hat{f}}[\hat{f}(x_S, X_S) - \mathbb{E}_{D|\hat{f}}[\hat{f}(X_S, X_S)]]$  instead (proof analogous to §A.5). Since centered ICE curves fulfill local decomposability [13], their variance at  $x_S$  is solely due to interactions involving feature  $X_S$ . Thus, the estimation variance of the centered PD is zero when  $X_S$  has no interactions in  $\hat{f}$ . An overview of all four derived error components is provided in Fig. 1.

## 4.2 Full Error Decomposition of the ALE Estimator

We now provide an error analysis for ALE, which is missing in the current literature. The MSE of  $\widehat{ALE}_{\hat{f}}$  w.r.t.  $ALE_f$  can be decomposed into bias and variance analogous to PD in Eq. (4) (proof in §A.2, analogous to the one for PD). The only property required for the argument is that all expectations exist and that  $f$ , and hence  $ALE_f$ , is non-random w.r.t. to  $\mathbb{P}_F$ . For the theoretical analysis

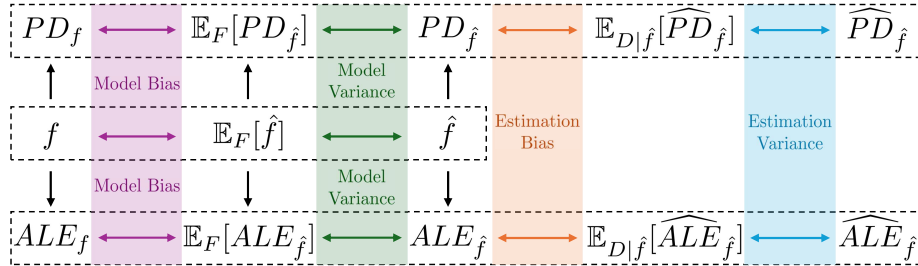


Fig. 1: Conceptual overview of the four error components.

of the error components, we focus on uncentered ALE, as centering is linear post-processing that only affects the offset. All sources of bias and variance originate in the uncentered ALE and propagate deterministically under centering.

**Bias.** Similar to PD, we can decompose the bias of ALE further into:

$$\begin{aligned} & \mathbb{E}_F \mathbb{E}_{D|\hat{f}}[\widehat{ALE}_{\hat{f}}(x_S)] - \widetilde{ALE}_f(x_S) = \\ & \mathbb{E}_F \left[ \mathbb{E}_{D|\hat{f}}[\widehat{ALE}_{\hat{f}}(x_S)] - \widetilde{ALE}_{\hat{f}}(x_S) \right] + (\mathbb{E}_F[\widetilde{ALE}_{\hat{f}}(x_S)] - \widetilde{ALE}_f(x_S)), \end{aligned} \quad (9)$$

by adding and subtracting  $\mathbb{E}_F[\widetilde{ALE}_{\hat{f}}(x_S)]$ . The first part can be viewed as the average “estimation bias” and can be further decomposed into:

$$\begin{aligned} & \mathbb{E}_F[\mathbb{E}_{D|\hat{f}}[\widehat{ALE}_{\hat{f}}(x_S)] - \widetilde{ALE}_{\hat{f}}(x_S)] = \\ & \mathbb{E}_F[\mathbb{E}_{D|\hat{f}}[\widehat{ALE}_{\hat{f}}(x_S)] - \widetilde{ALE}_{\hat{f}}^K(x_S)] + \mathbb{E}_F[\widetilde{ALE}_{\hat{f}}^K(x_S) - \widetilde{ALE}_{\hat{f}}(x_S)]. \end{aligned} \quad (10)$$

The first term is due to estimation on finite samples. For ALE estimation on holdout data, under mild regularity (Assumptions (iii) and (v)) and  $n_S(k) > 0$  for all relevant bins, the ALE estimator is unbiased w.r.t. the binned population ALE and the term becomes zero (proof in §A.6). To the second term, we refer as “discretization bias”: the term inside  $\mathbb{E}_F$  goes to 0 as  $K \rightarrow \infty$  (pointwise in  $\hat{f}$ ) by the definition of ALE (Eq. (2)). Convergence of the entire expectation term can be shown by applying the dominated convergence theorem exactly as in §A.7.

For the second part in Eq. (9), we show in §A.7 that it arises from an (infinite) sum of the local average biases in the finite differences of  $\hat{f}$  w.r.t. those of  $f$ . Thus, it vanishes when the model’s conditional finite differences are unbiased w.r.t. those of  $f$ . In particular, this is satisfied if  $\hat{f}$  is unbiased w.r.t.  $f$  for all  $\mathbf{x}$ .

**Model variance.** When ALE is estimated on holdout data, it holds that  $\text{Var}_F[\mathbb{E}_{D|\hat{f}}[\widehat{ALE}_{\hat{f}}(x_S)]] = \text{Var}_F[\widetilde{ALE}_{\hat{f}}^K(x_S)]$  by the ALE estimator’s unbiasedness (see above). For this expression, we obtain an upper bound for the variance of ALE w.r.t. the model distribution (proof in §A.8):

$$\text{Var}_F \left[ \widetilde{ALE}_{\hat{f}}^K(x_S) \right] \leq k_S(x_S) \sum_{k=1}^{k_S(x_S)} \mathbb{E}_{X_S|X_S \in I_S(k)} \text{Var}_F \left[ \Delta_{\hat{f}}(k, X_S) \right]. \quad (11)$$

Thus, the theoretical ALE variance at  $x_S$  is controlled by the local average variability of finite differences across models along the intervals up to  $x_S$ .

**Estimation variance.** By conditioning on the samples’ bin assignments,  $B = (B^{(1)}, \dots, B^{(n)})$  with  $B^{(i)} = k_S(X_S^{(i)})$ , and using the law of total variance, the estimation variance of ALE,  $\mathbb{E}_F[\text{Var}_{D|\hat{f}}[\widehat{ALE}_{\hat{f}}(x_S)]]$ , decomposes into

$$\mathbb{E}_F \left[ \text{Var}_{B|\hat{f}} \left[ \mathbb{E}_{D|\hat{f}, B} \left[ \widehat{ALE}_{\hat{f}}(x_S) \right] \right] \right] + \mathbb{E}_F \left[ \mathbb{E}_{B|\hat{f}} \left[ \text{Var}_{D|\hat{f}, B} \left[ \widehat{ALE}_{\hat{f}}(x_S) \right] \right] \right].$$

Table 1: Estimators of the feature effect error components at  $x_S$ .

Component	Estimator
MSE	$\widehat{\text{MSE}}(x_S) = \frac{1}{M} \sum_{m=1}^M (PD_f(x_S) - \widehat{PD}_{\hat{f}^{(m)}}(x_S))^2$
Bias	$\widehat{\text{Bias}}(x_S) = PD_f(x_S) - \frac{1}{M} \sum_{m=1}^M \widehat{PD}_{\hat{f}^{(m)}}(x_S)$
Variance	$\widehat{\text{Var}}(x_S) = \frac{1}{M-1} \sum_{m=1}^M \left( \widehat{PD}_{\hat{f}^{(m)}}(x_S) - \frac{1}{M} \sum_{m'=1}^M \widehat{PD}_{\hat{f}^{(m')}}(x_S) \right)^2$
Estimation variance	$\widehat{\text{Var}}_{\text{Est}}(x_S) = \frac{1}{M(R-1)} \sum_{m=1}^M \sum_{r=1}^R \left( \widehat{PD}_{\hat{f}^{(m)}}^{[r]}(x_S) - \frac{1}{R} \sum_{r'=1}^R \widehat{PD}_{\hat{f}^{(m)}}^{[r']}(x_S) \right)^2$

The first term captures variance from random bin assignments along  $X_S$ , i.e., variability in the expected ALE estimate due to random sample allocation to bins. For the second term, assuming  $n_S(k) > 0$  for all relevant bins  $k \leq k_S(x_S)$ :

$$\mathbb{E}_F \mathbb{E}_{B|\hat{f}} \text{Var}_{D|\hat{f}, B} \left[ \widehat{\text{ALE}}_{\hat{f}}(x_S) \right] = \sum_{k \leq k_S(x_S)} \mathbb{E}_F \mathbb{E}_{B|\hat{f}} \left[ \frac{1}{n_S(k)} \sigma_k^2(\hat{f}) \right] \quad (12)$$

with  $\sigma_k^2(\hat{f}) := \text{Var}_{X_{\bar{S}}|X_S \in I_S(k), \hat{f}}[\Delta_{\hat{f}}(k, X_{\bar{S}})]$ . The proof is given in §A.9. Thus, it scales with the expected inverse number of observations per bin. Assuming deterministic equal-frequency binning for simplicity, this factor becomes  $\frac{K}{n}$ . It also depends on the local variance in the estimated finite differences. Finite differences also fulfill local decomposability [13]. Thus, the variance  $\sigma_k^2(\hat{f})$  is only due to interaction effects involving feature  $X_S$  and is zero when  $X_S$  has no interaction effects in  $\hat{f}$ .

### 4.3 Estimators of the Error Components

To investigate the error components empirically in §5-6, we propose estimators for each.  $\mathbb{E}_F$  and  $\text{Var}_F$  can be estimated by averaging over multiple models  $\hat{f}^{(m)}$  of the same learner fitted to  $M$  different training sets, each independently sampled from  $\mathbb{P}_{XY}$ . Translating the standard estimators for MSE, bias, and variance [20] to our setting yields the estimators in Tab. 1. The variance estimator is the same as in [17], capturing the variance in both model fits and Monte Carlo integration. To estimate the estimation variance separately, consider  $R$  Monte Carlo iterations  $\mathcal{D}_r$  to estimate the feature effect  $\widehat{PD}_{\hat{f}^{(m)}}^{[r]}$ , again for multiple model refits. While Tab. 1 is based on PD, estimators for ALE follow analogously.

These estimators are unbiased according to standard statistical results. The Monte Carlo standard errors of these estimates can again be estimated as a function of the number of repetitions [20]. Importantly, most estimators in Tab. 1 are impractical as they require knowledge of the ground-truth. We will rather use them to understand the behavior of feature effect estimation.

## 5 Experimental Set-Up

We now empirically validate our findings from §4 with an extensive simulation study. While the theoretical analysis requires holdout data at multiple points

Table 2: Data settings with underlying functions and feature structure.

Setting	Function	Correlation
<b>Simple-Normal-Correlated</b>	$f_1(\mathbf{x}) = x_1 + \frac{x_2^2}{2} + x_1x_2$	$X_1, \dots, X_4 \sim N(0, 1), \rho_{12} = 0.9,$ $\rho_{ij} = 0 \forall (i, j) \neq (1, 2), i \neq j$
<b>Friedman1</b> [6]	$f_2(\mathbf{x}) = 10 \sin(\pi x_1 x_2)$ $+ 20(x_3 - \frac{1}{2})^2 + 10x_4 + 5x_5$	$X_1, \dots, X_7 \stackrel{\text{i.i.d.}}{\sim} U(0, 1)$
<b>Feynman I.29.16</b> [15]	$f_3(\mathbf{x}, \theta) = \sqrt{x_1^2 + x_2^2 + 2x_1x_2 \cos(\theta_1 - \theta_2)}$	$X_1, X_2 \sim \text{LogU}(0.1, 10),$ $\theta_1, \theta_2 \sim U(0, 2\pi),$ $D_1, D_2 \sim U(0, 1), \text{ all indep.}$

(e.g., to avoid estimation bias), we aim to gain deeper insights into what empirically happens when this is violated. For this, we compare feature effect errors across different estimation strategies: on training data, validation data, and via CV. We break this overarching goal down into three specific research questions:

**RQ1:** How does overfitting empirically affect MSE, bias, and variance of PD and ALE when estimated on training vs. validation data vs. CV?

**RQ2:** How do the variance sources (model and estimation variance) empirically behave for PD and ALE on training vs. validation data vs. in CV?

**RQ3:** How does sample size affect estimation error for PD and ALE empirically?

**Data settings.** We consider three settings of varying complexity. Ground-truth functions and feature structures are given in Tab. 2. All settings include two independent dummy features. The first setting has correlations and interactions, the second different non-linearities, and the third real-world relevance.<sup>8</sup> Features are generated i.i.d., and the target as  $y = f(\mathbf{x}) + \varepsilon$  with i.i.d.  $\varepsilon \sim \mathcal{N}(0, \sigma_\varepsilon^2)$  and a signal-to-noise ratio of 5.<sup>9</sup> We consider two sample sizes  $n = 1250$  and  $n = 10000$ .

**Models.** We consider a generalized additive model (GAM) with spline bases for main and pairwise interaction effects, and XGBoost as learners. Each of them is once configured with “optimally tuned” (OT) hyperparameters and once with hyperparameters chosen to overfit (OF). These hyperparameters are pre-selected per setting and sample size, i.e., carefully hand-picked for OF (e.g., small penalty / large learning rate) and tuned on separate data samples for OT. For details on the hyperparameters and model performances, see §B.1.

**Feature effect estimation.** We estimate the feature effects  $\widehat{PD}_{\hat{f}}$  and  $\widehat{ALE}_{\hat{f}}$  per feature and model by (a) training a model on all  $n$  samples and estimating the feature effect on the same  $n$  samples, (b) splitting the  $n$  samples into 80% train and 20% validation set, fitting a model on the training set and estimating the effect on the validation set, and (c) a CV-based estimation strategy on all  $n$  samples.<sup>10</sup> We compute feature effects all at the same 100 grid points, defined

<sup>8</sup> This dataset is based on the physics-grounded Feynman equation I.29.16 for wave interference, addressing the limited realism of standard test functions.

<sup>9</sup> The scale parameter is set such that  $\hat{\sigma}_Y / \sigma_\varepsilon = 5$ .

<sup>10</sup> We use 5-fold CV: in each iteration, a model is fitted on four folds, effects are estimated on the held-out fold, and the five resulting effects are averaged pointwise.

by the theoretical quantiles of  $\mathbb{P}_{X_S}$  for comparability. Additionally, we center the curves after estimation, and omit the first and last grid point to avoid boundary effects, particularly for ALE. To enable ground-truth comparisons, we additionally construct ground-truth effect estimators in the same manner, but on 10,000 fresh samples and directly on  $f$ . This eliminates the discretization bias from our error, as the ground-truth and estimate use the same intervals.<sup>11</sup>

**Experiments.** To address RQ1, we compute the MSE, bias, and variance of all estimated model feature effects w.r.t. the estimated ground-truth effects via the estimators in Tab. 1 with  $\widehat{PD}_f$  for  $PD_f$  (analog. for ALE). We repeat each setting-size-model combination  $M = 30$  times to estimate the error terms. Each repetition involves drawing new data, fitting the models, and estimating the effects. We report MSE, bias, and variance averaged over the grid points.

To address RQ2, we estimate the estimation variance according to Tab. 1. In each iteration  $m \in \{1, \dots, M\}$ , we fix the trained models, draw  $R = 30$  new data sets, and estimate the effects with them for the fixed models. By subtracting this from the total variance (cf. RQ1), we estimate the model variance. For this analysis, we focus on XGBoost (OF & OT) and a sample size of  $n = 1250$ .

To address RQ3, we compute the MSE between analytical ground-truth effects (available for the first two settings) and estimated ground-truth effects across 50 different sample sizes ranging from  $10^1$  to  $10^6$  (on log scale) with 50 repetitions per size. This isolates the estimation error, as no model is involved.

**Reproducibility.** Experiments are implemented in Python and use fixed random seeds. We release all experimental code and raw results on GitHub ([link](#)).

## 6 Empirical Results

We report results for a single setting and a representative feature subset. Further results are provided in §B.2 and consistent with the findings reported here.

### 6.1 Bias-Variance-Analysis

**PD decomposition.** Our empirical results on *SimpleNormalCorrelated* in Tab. 3 reveal that the MSE of the PD estimator is lowest mostly for CV- and training-set-based estimation. Bias is mostly similar across the estimation strategies, and we observe no systematic trends w.r.t. estimation strategy or sample size. Thus, a potential bias introduced by estimation on training data that could not be ruled out in our theoretical analysis (§4.1) appears empirically negligible. Variance is generally lowest for CV-based estimation. We hypothesize that this is due to two effects: (1) model variance may decrease as CV averages out fitting variability across multiple models, and (2) estimation variance may decrease compared to estimation on a single validation set due to increased effective sample size. Variance is generally slightly higher for validation than for training-set-based

<sup>11</sup> Except for discretization bias, this estimate is unbiased w.r.t. the true theoretical effect (cf. §4), and adds negligible estimation variance at this sample size (cf. §6.3).

Table 3: Results for PD on *SimpleNormalCorrelated* averaged over 100 grid points. Bold numbers are minimum per metric-feature-model-size-combination.

		Feature Metric	MSE	$x_1$ Bias	Var	MSE	$x_2$ Bias	Var	MSE	$x_3$ Bias	Var
$n = 1250$	GAM_OF	train	0.0695	0.0296	0.0710	0.0699	<b>0.0276</b>	0.0716	0.0090	0.0161	0.0091
		val	0.0928	<b>0.0206</b>	0.0955	0.0849	0.0345	0.0865	0.0114	0.0190	0.0114
		CV	<b>0.0609</b>	0.0264	<b>0.0622</b>	<b>0.0562</b>	0.0292	<b>0.0573</b>	<b>0.0086</b>	<b>0.0157</b>	<b>0.0086</b>
	GAM_OT	train	<b>0.0051</b>	<b>0.0323</b>	0.0042	<b>0.0039</b>	<b>0.0247</b>	<b>0.0034</b>	0.0005	<b>0.0022</b>	0.0005
		val	0.0089	0.0336	0.0081	0.0093	0.0305	0.0086	0.0005	0.0040	0.0005
		CV	0.0053	0.0356	<b>0.0042</b>	0.0041	0.0287	0.0034	<b>0.0005</b>	0.0022	<b>0.0005</b>
	XGB_OF	train	0.1780	0.3147	0.0817	0.4217	0.4505	0.2263	0.0010	0.0043	0.0010
		val	0.1880	0.3242	0.0857	0.3888	<b>0.3941</b>	0.2416	0.0015	0.0098	0.0014
		CV	<b>0.1458</b>	<b>0.3114</b>	<b>0.0505</b>	<b>0.3043</b>	0.4236	<b>0.1291</b>	<b>0.0007</b>	<b>0.0042</b>	<b>0.0007</b>
XGB_OT	train	<b>0.2807</b>	<b>0.5194</b>	0.0113	0.1690	0.3941	0.0141	0.0014	0.0052	0.0014	
	val	0.3008	0.5375	0.0123	<b>0.1666</b>	<b>0.3894</b>	0.0155	0.0019	0.0073	0.0019	
	CV	0.2950	0.5351	<b>0.0090</b>	0.1691	0.3987	<b>0.0104</b>	<b>0.0013</b>	<b>0.0051</b>	<b>0.0013</b>	
$n = 10000$	GAM_OF	train	0.1878	0.0674	0.1895	0.1995	0.0890	0.1982	0.0008	0.0050	0.0008
		val	0.2248	<b>0.0601</b>	0.2289	0.2371	<b>0.0678</b>	0.2406	0.0011	0.0055	0.0011
		CV	<b>0.1777</b>	0.0778	<b>0.1775</b>	<b>0.1875</b>	0.0996	<b>0.1837</b>	<b>0.0008</b>	<b>0.0050</b>	<b>0.0008</b>
	GAM_OT	train	<b>0.0011</b>	<b>0.0206</b>	0.0007	<b>0.0012</b>	<b>0.0204</b>	0.0008	0.0000	<b>0.0009</b>	0.0000
		val	0.0020	0.0228	0.0016	0.0018	0.0222	0.0014	0.0001	0.0012	0.0001
		CV	0.0012	0.0232	<b>0.0007</b>	0.0013	0.0230	<b>0.0008</b>	<b>0.0000</b>	0.0010	<b>0.0000</b>
	XGB_OF	train	0.0915	<b>0.2638</b>	0.0227	0.2625	0.4404	0.0710	0.0003	0.0029	0.0003
		val	0.1029	0.2675	0.0324	0.2700	0.4465	0.0730	0.0004	0.0037	0.0004
		CV	<b>0.0828</b>	0.2641	<b>0.0135</b>	<b>0.2226</b>	<b>0.4277</b>	<b>0.0411</b>	<b>0.0002</b>	<b>0.0022</b>	<b>0.0002</b>
XGB_OT	train	<b>0.1752</b>	<b>0.4142</b>	0.0037	<b>0.1210</b>	<b>0.3418</b>	0.0043	0.0002	0.0022	0.0002	
	val	0.1802	0.4197	0.0042	0.1226	0.3439	0.0045	0.0003	0.0022	0.0003	
	CV	0.1806	0.4215	<b>0.0030</b>	0.1237	0.3471	<b>0.0033</b>	<b>0.0002</b>	<b>0.0021</b>	<b>0.0002</b>	

estimation, likely due to the smaller sample size. The higher variance of overfitting models reflects in higher PD variance. These empirical results agree with our theoretical findings. An additional finding is that, for well-generalizing models, differences in MSE across estimation strategies are mostly negligible, while for overfitting models, CV-based estimation yields a substantial reduction.

**ALE decomposition.** Similar results for ALE in Tab. 4 show that the MSE is again lowest for training-set- or CV-based estimation. In contrast to PD, bias is often considerably lower for training data (largest set) when  $n$  is small, and generally decreases with increasing sample size, likely as the probability of  $n_S(k) > 0 \forall k$  grows (required for unbiasedness, cf. §4.2). Again, the variance is mostly lowest for CV-based estimation, but now substantially higher on the smaller validation set, supporting our theoretical result that ALE (estimation) variance is more sensitive to sample size than PD. Generally, this confirms our theoretical findings and again shows that CV-based estimation is promising.

## 6.2 Variance Decomposition Analysis

For variance decomposition into model and estimation variance, we consider the results on *Friedman1* in Tab. 5, including a non-linear feature with interactions ( $X_1$ ), a linear without ( $X_4$ ), and a dummy feature ( $X_7$ ). The estimation variance is constantly highest when feature effects are estimated on the smaller validation set. This is more pronounced for ALE, and we generally observe higher

Table 4: Results for ALE on *SimpleNormalCorrelated* averaged over 100 grid points. Bold numbers are minimum per metric-feature-model-size-combination.

		Feature Metric	MSE	$x_1$ Bias	Var	MSE	$x_2$ Bias	Var	MSE	$x_3$ Bias	Var
$n = 1250$	GAM_OF	train	<b>0.0123</b>	<b>0.0205</b>	0.0123	<b>0.0108</b>	<b>0.0236</b>	<b>0.0106</b>	0.0091	0.0161	0.0092
		val	0.0277	0.0771	0.0225	0.0304	0.0711	0.0262	0.0129	0.0176	0.0131
		CV	0.0178	0.0857	<b>0.0108</b>	0.0190	0.0858	0.0120	<b>0.0077</b>	<b>0.0153</b>	<b>0.0077</b>
	GAM_OT	train	<b>0.0022</b>	<b>0.0100</b>	<b>0.0021</b>	<b>0.0019</b>	<b>0.0061</b>	<b>0.0019</b>	0.0005	0.0022	0.0005
		val	0.0148	0.0808	0.0086	0.0198	0.0918	0.0117	0.0005	0.0036	0.0005
		CV	0.0103	0.0899	0.0023	0.0109	0.0890	0.0031	<b>0.0004</b>	<b>0.0020</b>	<b>0.0004</b>
	XGB_OF	train	<b>0.1159</b>	0.1343	<b>0.1012</b>	0.1120	0.1196	0.1011	0.0724	0.0279	0.0741
		val	0.5238	0.1153	0.5281	0.6017	0.1415	0.6017	0.0848	0.0354	0.0864
		CV	0.1531	<b>0.0784</b>	0.1520	<b>0.1025</b>	<b>0.0803</b>	<b>0.0994</b>	<b>0.0118</b>	<b>0.0126</b>	<b>0.0121</b>
XGB_OT	train	<b>0.0162</b>	<b>0.0875</b>	0.0088	<b>0.0174</b>	<b>0.0768</b>	0.0119	0.0065	0.0077	0.0066	
	val	0.0471	0.1470	0.0263	0.0386	0.1094	0.0275	0.0033	0.0116	0.0033	
	CV	0.0315	0.1549	<b>0.0077</b>	0.0234	0.1158	<b>0.0103</b>	<b>0.0020</b>	<b>0.0053</b>	<b>0.0020</b>	
$n = 10000$	GAM_OF	train	0.0011	0.0071	0.0011	0.0012	<b>0.0071</b>	0.0011	0.0008	<b>0.0050</b>	0.0008
		val	0.0017	0.0075	0.0017	0.0017	0.0085	0.0017	0.0011	0.0057	0.0011
		CV	<b>0.0011</b>	<b>0.0068</b>	<b>0.0011</b>	<b>0.0011</b>	0.0072	<b>0.0011</b>	<b>0.0008</b>	0.0050	<b>0.0008</b>
	GAM_OT	train	0.0002	0.0030	0.0002	0.0003	<b>0.0045</b>	0.0002	<b>0.0000</b>	<b>0.0009</b>	0.0000
		val	0.0006	0.0037	0.0006	0.0005	0.0056	0.0005	0.0001	0.0012	0.0001
		CV	<b>0.0002</b>	<b>0.0029</b>	<b>0.0002</b>	<b>0.0003</b>	0.0046	<b>0.0002</b>	0.0000	0.0010	<b>0.0000</b>
	XGB_OF	train	0.0164	0.0346	0.0157	0.0197	0.0520	0.0176	0.0103	0.0189	0.0103
		val	0.0652	0.0416	0.0657	0.0780	0.0597	0.0770	0.0155	0.0166	0.0157
		CV	<b>0.0130</b>	<b>0.0180</b>	<b>0.0131</b>	<b>0.0147</b>	<b>0.0198</b>	<b>0.0148</b>	<b>0.0023</b>	<b>0.0098</b>	<b>0.0023</b>
XGB_OT	train	0.0046	<b>0.0538</b>	0.0017	0.0039	<b>0.0401</b>	0.0023	0.0005	0.0037	0.0005	
	val	0.0054	0.0544	0.0025	0.0047	0.0412	0.0031	0.0006	0.0037	0.0007	
	CV	<b>0.0044</b>	0.0555	<b>0.0014</b>	<b>0.0034</b>	0.0417	<b>0.0017</b>	<b>0.0003</b>	<b>0.0027</b>	<b>0.0003</b>	

estimation variance than for PD. As hypothesized, CV (1) reduces model variance compared to the other estimation strategies, which is most pronounced for overfitting models (generally higher model variance). As expected, it also (2) reduces estimation variance compared to a single validation set. These empirical findings agree with our theoretical results. Although estimation variance is sometimes slightly higher for features with interactions ( $X_1$ ), XGBoost may also learn interactions that are not in  $f$ , which is why this is not as clear as expected.

### 6.3 Effect of the Sample Size

Our results for the effect of sample size are shown in Fig. 2 for *Friedman1*. For PD on holdout data, we know that there is no estimation bias (cf. §4.1) and Fig. 2a contains only estimation variance. We observe the expected polynomial decrease at roughly  $1/n$  for features with interactions ( $X_1$ ) and a negligible error across sample sizes for features without interactions ( $X_4$ ), as expected for centered PD.

For ALE, we know from §4.2 that there are also estimation biases in addition to variance due to discretization and when  $n_S(k) = 0$ . With interactions ( $X_1$ ), the observed estimation error in Fig. 2b is closer to  $K/n$  for small sample sizes but gets closer to  $1/n$  as the sample size increases. For features without interactions, we observe a sharp drop in the estimation error at  $n = K$ , reducing it to the expected negligible level. This may be due to reduced estimation bias at this sample size, as each interval could, in principle, now contain at least one sample.

Table 5: Decomposition results of total variance  $\text{Var}_{\text{Tot}}$  into model variance  $\text{Var}_{\text{Mod}}$  and estimation variance  $\text{Var}_{\text{Est}}$  on *Friedman1* averaged over 100 grid points. Bold numbers indicate estimation strategy with minimal variance.

	Feature Metric	$x_1$			$x_4$			$x_7$			
		$\text{Var}_{\text{Tot}}$	$\text{Var}_{\text{Mod}}$	$\text{Var}_{\text{Est}}$	$\text{Var}_{\text{Tot}}$	$\text{Var}_{\text{Mod}}$	$\text{Var}_{\text{Est}}$	$\text{Var}_{\text{Tot}}$	$\text{Var}_{\text{Mod}}$	$\text{Var}_{\text{Est}}$	
PD	XGB_OF	train	0.0862	0.0833	0.0029	0.1269	0.1240	0.0029	0.0027	0.0025	0.0002
		val	0.1120	0.0974	0.0146	0.1811	0.1661	0.0150	0.0059	0.0046	0.0012
		CV	<b>0.0460</b>	<b>0.0432</b>	<b>0.0028</b>	<b>0.0814</b>	<b>0.0785</b>	<b>0.0029</b>	<b>0.0014</b>	<b>0.0011</b>	<b>0.0002</b>
	XGB_OT	train	0.0217	0.0209	<b>0.0008</b>	0.0232	0.0231	0.0001	0.0071	0.0070	<b>0.0000</b>
		val	0.0280	0.0241	0.0038	0.0283	0.0278	0.0006	0.0083	0.0082	0.0001
		CV	<b>0.0190</b>	<b>0.0182</b>	0.0008	<b>0.0205</b>	<b>0.0204</b>	<b>0.0001</b>	<b>0.0062</b>	<b>0.0062</b>	0.0000
ALE	XGB_OF	train	1.0248	0.4286	0.5962	1.1178	0.4220	<b>0.6958</b>	0.1852	0.1556	0.0296
		val	4.6600	1.5201	3.1399	4.9819	1.1399	3.8420	0.3004	0.1614	0.1390
		CV	<b>0.6573</b>	<b>0.0846</b>	<b>0.5727</b>	<b>0.8568</b>	<b>0.0858</b>	0.7710	<b>0.0262</b>	*	<b>0.0287</b>
	XGB_OT	train	0.0337	0.0229	<b>0.0108</b>	0.0340	0.0265	<b>0.0075</b>	0.0125	0.0113	<b>0.0012</b>
		val	0.0937	0.0200	0.0737	0.1113	0.0463	0.0651	0.0154	0.0075	0.0080
		CV	<b>0.0299</b>	<b>0.0147</b>	0.0151	<b>0.0273</b>	<b>0.0143</b>	0.0129	<b>0.0067</b>	<b>0.0051</b>	0.0016

\* Due to instabilities in variance estimation for ALE, likely caused by unstable bin assignments, the estimated  $\text{Var}_{\text{Est}}$  sometimes exceeds the estimated  $\text{Var}_{\text{Tot}}$ . We omit  $\text{Var}_{\text{Mod}}$  in these cases.

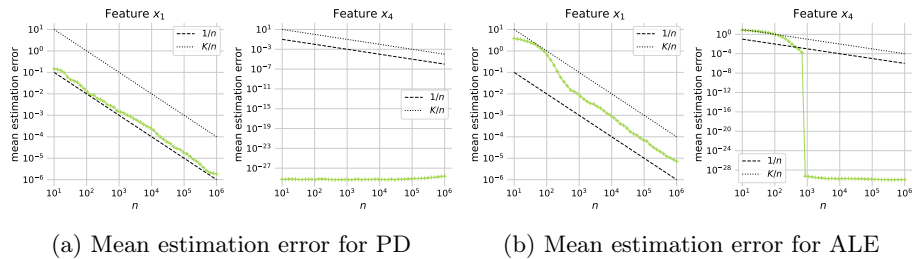


Fig. 2: Mean estimation errors on *Friedman1* for  $X_1$  and  $X_4$ . For each sample size  $n$ , the variances are averaged over all grid points. Both axes are log-scale.

## 7 Conclusion & Future Work

**Summary.** In this work, we presented an estimator-level analysis of global feature effect estimation for PD and ALE. We derived a full MSE decomposition that separates model bias, estimation bias, model variance, and estimation variance, and we analyzed these components theoretically. Our results show that the model bias component follows directly from systematic biases in the model  $\hat{f}$  for PD or in the finite differences of  $\hat{f}$  for ALE. For PD, the estimation bias is zero on holdout data. For ALE, it consists of a bias when  $n_S(k) = 0$ , and a discretization bias due to binning. For both PD and ALE, we derived upper bounds on the model variance in terms of pointwise variance of  $\hat{f}$  (PD) or its finite differences (ALE). Estimation variance is governed by (1) the sample size, scaling as  $1/n$  for PD and as the expected inverse bin counts for ALE, explaining ALE’s sensitivity in small-sample regimes, and (2) the variance of the ICE curves / finite differences. For centered PD and generally for ALE, the latter depends only on interactions with  $X_S$ .

We validated our theoretical findings through simulations by comparing feature effect estimation on training and validation data and a CV-based strategy. Our empirical results showed that potential bias from estimating feature effects on the training data is negligible across our settings, including when models overfit (RQ1). Differences are instead dominated by sample-size effects: validation-set-based estimation yields higher variance (for ALE also higher bias), while training-set- and CV-based estimation attain the lowest MSE. Variance decomposition (RQ2) shows that the estimation variance is consistently highest on the smaller validation set and more pronounced for ALE, in line with our theoretical results. CV reduces model variance by averaging across fits (particularly beneficial for overfitting models) and estimation variance through a higher effective sample size compared to a single validation set. The observed estimation error (RQ3) confirms our theoretical results on sample size and interaction effects.

**Practical implications.** While using holdout data is theoretically cleaner, our results indicate that training-set-based feature effect estimation is empirically safe and often preferable because it has a larger sample size. CV-based estimation emerges as a robust alternative, particularly for overfitting models. Although such models are typically identified via appropriate performance estimation and ruled out, this may not always be perfectly possible in all applications, in which cases CV-based feature effect estimation can be a safer option.

**Limitations & future work.** Our empirical results are themselves estimates with errors from finite repetitions, which can lead to artifacts, such as estimation variance estimates exceeding total variance (cf. Tab. 5). Additionally, the empirical analysis considers only low-dimensional settings and two model classes. Further, our theoretical analysis leaves room for future research, including: (1) a tighter bias analysis for cases in which  $D \perp \hat{f}$  does not hold to formalize what happens for training-set-based estimation, (2) a formal theory for CV-based estimation results, (3) extensions of our analysis to distribution shifts between training and estimation data, which is another practically relevant issue.

## References

1. Apley, D.W., Zhu, J.: Visualizing the effects of predictor variables in black box supervised learning models. *Journal of the Royal Statistical Society Series B: Statistical Methodology* **82**(4), 1059–1086 (2020)
2. Bergstra, J., Bardenet, R., Bengio, Y., Kégl, B.: Algorithms for hyper-parameter optimization. In: *Proceedings of the 25th International Conference on Neural Information Processing Systems*. p. 2546–2554. NIPS’11, Curran Associates Inc., Red Hook, NY, USA (2011)
3. Chang, C.Y., Chang, M.C.: Accelerated aggregated D-optimal designs for estimating main effects in black-box models. *arXiv:2510.08465 [stat.ML]* (2025)
4. Chen, T., Guestrin, C.: XGBoost: A scalable tree boosting system. In: *Proceedings of the 22nd ACM SIGKDD International Conference on Knowledge Discovery and Data Mining*. p. 785–794. KDD ’16, ACM, New York, NY, USA (2016)
5. Cook, T.R., Modig, Z.D., Palmer, N.M.: Explaining machine learning by bootstrapping partial marginal effects and Shapley values. *FEDS Working Paper No. 2024-75* (2024)

6. Friedman, J.H.: Multivariate adaptive regression splines. *The Annals of Statistics* **19**(1), 1–67 (1991), publisher: Institute of Mathematical Statistics
7. Friedman, J.H.: Greedy function approximation: A gradient boosting machine. *The Annals of Statistics* **29**(5), 1189–1232 (2001)
8. Gkolemis, V., Dalamagas, T., Diou, C.: DALE: Differential accumulated local effects for efficient and accurate global explanations. In: *Proceedings of The 14th Asian Conference on Machine Learning*, pp. 375–390. PMLR (2023)
9. Gkolemis, V., Dalamagas, T., Ntoutsis, E., Diou, C.: RHALE: Robust and heterogeneity-aware accumulated local effects. In: *ECAI 2023*, pp. 859–866. IOS Press (2023)
10. Goldstein, A., Kapelner, A., Bleich, J., Pitkin, E.: Peeking inside the black box: Visualizing statistical learning with plots of individual conditional expectation. *Journal of Computational and Graphical Statistics* **24**(1), 44–65 (2015)
11. Greenwell, B.: pdp: An R package for constructing partial dependence plots. *The R Journal* **9**/1 (2017)
12. Herbringer, J., Bischl, B., Casalicchio, G.: REPID: Regional effect plots with implicit interaction detection. In: *Proceedings of The 25th International Conference on Artificial Intelligence and Statistics*, pp. 10209–10233. PMLR (2022)
13. Herbringer, J., Wright, M.N., Nagler, T., Bischl, B., Casalicchio, G.: Decomposing global feature effects based on feature interactions. *Journal of Machine Learning Research* **25**(381), 1–65 (2024)
14. Loecher, M.: Debiasing MDI feature importance and SHAP values in tree ensembles. In: *Holzinger, A., Kieseberg, P., Tjoa, A.M., Weippl, E. (eds.) Machine Learning and Knowledge Extraction*, pp. 114–129. Springer International Publishing, Cham (2022)
15. Matsubara, Y., Chiba, N., Igarashi, R., Ushiku, Y.: Rethinking symbolic regression datasets and benchmarks for scientific discovery. *Journal of Data-centric Machine Learning Research* **1** (2024)
16. Molnar, C.: *Interpretable machine learning: a guide for making black box models explainable*. Christoph Molnar, Munich, Germany, 2nd edn. (2022)
17. Molnar, C., Freiesleben, T., König, G., Herbringer, J., Reisinger, T., Casalicchio, G., Wright, M.N., Bischl, B.: Relating the partial dependence plot and permutation feature importance to the data generating process. In: *Longo, L. (ed.) Explainable Artificial Intelligence*, pp. 456–479. Springer Nature Switzerland, Cham (2023)
18. Molnar, C., König, G., Herbringer, J., Freiesleben, T., Dandl, S., Scholbeck, C.A., Casalicchio, G., Grosse-Wentrup, M., Bischl, B.: General pitfalls of model-agnostic interpretation methods for machine learning models. In: *Holzinger, A., Goebel, R., Fong, R., Moon, T., Müller, K.R., Samek, W. (eds.) xxAI - Beyond Explainable AI: International Workshop, Held in Conjunction with ICML 2020, July 18, 2020, Vienna, Austria, Revised and Extended Papers*, pp. 39–68. Springer International Publishing, Cham (2022)
19. Moosbauer, J., Herbringer, J., Casalicchio, G., Lindauer, M., Bischl, B.: Explaining hyperparameter optimization via partial dependence plots. In: *Proceedings of the 35th International Conference on Neural Information Processing Systems. NIPS '21, Curran Associates Inc., Red Hook, NY, USA* (2021)
20. Morris, T.P., White, I.R., Crowther, M.J.: Using simulation studies to evaluate statistical methods. *Statistics in Medicine* **38**(11), 2074–2102 (2019)
21. Probst, P., Boulesteix, A.L., Bischl, B.: Tunability: Importance of hyperparameters of machine learning algorithms. *Journal of Machine Learning Research* **20**(53), 1–32 (2019)
22. Servén, D., Brummitt, C.: *pygam: Generalized additive models in python* (2018)

## Appendix

### A Theoretical Evidence

#### A.1 Assumptions

- (i) *Independence of feature effect definition and model.* Feature effects (both PD and ALE) are defined using expectations independent of the randomness in the training of  $\hat{f} \sim \mathbb{P}_F$ , meaning  $X_{\bar{S}} \perp \hat{f}$  for the theoretical PD / ALE.
- (ii) *Integrability of  $\hat{f}$  and  $f$ .* For all features  $X_S$  and points  $x_S$ , the random variable  $\hat{f}(x_S, X_{\bar{S}})$  is integrable and square-integrable under the joint law  $\mathbb{P}_{(F, X_{\bar{S}})}$ , i.e.,  $\mathbb{E}_{(F, X_{\bar{S}})}[|\hat{f}(x_S, X_{\bar{S}})|] < \infty$  and  $\mathbb{E}_{(F, X_{\bar{S}})}[\hat{f}(x_S, X_{\bar{S}})^2] < \infty$ . In particular, this implies that for  $\mathbb{P}_F$ -almost all realizations of  $\hat{f}$  we have  $\mathbb{E}_{X_{\bar{S}}|\hat{f}}[\hat{f}(x_S, X_{\bar{S}})^2] < \infty$  by Tonelli's theorem for conditional probabilities / stochastic kernels (since  $\hat{f}(x_S, X_{\bar{S}})^2 \geq 0$ ). Likewise  $\mathbb{E}_{X_{\bar{S}}|\hat{f}}[|\hat{f}(x_S, X_{\bar{S}})|] < \infty$ . Analogously,  $f(x_S, X_{\bar{S}})$  is integrable and square-integrable under  $\mathbb{P}_{X_{\bar{S}}}$ , i.e.,  $\mathbb{E}_{X_{\bar{S}}}[|f(x_S, X_{\bar{S}})|] < \infty$  and  $\mathbb{E}_{X_{\bar{S}}}[f(x_S, X_{\bar{S}})^2] < \infty$ . These conditions hold in particular for the special case that  $X_{\bar{S}}$  and  $\hat{f}$  are independent, e.g., under Assumption (i). They ensure that the relevant expectations and variances are well defined (i.p., PD, ALE, and their estimators) and justify interchanging the order of integration (Fubini/Tonelli) where needed.
- (iii) *Finite conditional probabilities.* For all bins  $I_S(k)$  considered,  $\mathbb{P}(X_S \in I_S(k)) > 0$ , and the conditional law  $\mathbb{P}_{X_{\bar{S}}|X_S \in I_S(k)}$  is well-defined.
- (iv) *Uniform bounded total variation in  $x_S$ .* For all features  $X_S$ , there exists a nonnegative random variable  $V(\hat{f})$  such that, with probability 1 over  $\hat{f} \sim \mathbb{P}_F$ ,

$$\operatorname{ess\,sup}_{\mathbf{x}_S} \operatorname{TV}(t \mapsto \hat{f}(t, \mathbf{x}_{\bar{S}})) \leq V(\hat{f}), \quad \mathbb{E}_F[V(\hat{f})] < \infty.$$

- (v) *Integrability of finite differences.* For all features  $X_S$ , all  $K$  and all  $k$  considered, the finite differences of  $\hat{f}$  are integrable and square-integrable w.r.t. the joint law given the  $k$ -th bin, i.e., under  $\mathbb{P}_{(F, X)|X_S \in I_S^K(k)}$ . In other words,  $\mathbb{E}_{(F, X)|X_S \in I_S^K(k)}[\Delta_{\hat{f}, S}^K(k, X_{\bar{S}})^2] < \infty$ , and analogously to (ii) this implies  $\mathbb{E}_{X_{\bar{S}}|X_S \in I_S^K(k), \hat{f}}[\Delta_{\hat{f}, S}^K(k, X_{\bar{S}})^2] < \infty$  for  $\mathbb{P}_F$ -almost all  $\hat{f}$ . For integrability, we likewise have  $\mathbb{E}_{(F, X)|X_S \in I_S^K(k)}[|\Delta_{\hat{f}, S}^K(k, X_{\bar{S}})|] < \infty$ . Note that this follows from (iv) plus the square-integrability condition in (ii). As in (ii), the same integrability conditions hold for  $\Delta_{f, S}^K(k, X_{\bar{S}})$  (with  $f$  in place of  $\hat{f}$ ).
- (vi) *Existence and square-integrability of ALE targets.* For all features  $X_S$  and  $h \in \{\hat{f}, f\}$ , the theoretical uncentered ALE  $\widehat{ALE}_h(x_S)$  (Eq. (2)) exists for all  $x_S$ . Moreover, the centered theoretical ALE  $ALE_h(x_S)$  exists and has finite second moment w.r.t.  $X_S$ , i.e.,  $\mathbb{E}_{X_S}[ALE_h(X_S)^2] < \infty$ .

### A.2 Bias-Variance-Decomposition of the Estimators (Eq. (4))

*Proof.* Fix a feature index  $S$  and an evaluation point  $x_S$ . Let  $D$  denote a random dataset used to estimate the feature effect. For better readability, we omit the point  $x_S$ . Under Assumption (ii) for either dependent or independent  $D$  and  $\hat{f}$ ,

$$\begin{aligned}
 \mathbb{E}_F \mathbb{E}_{D|\hat{f}}[(PD_f - \widehat{PD}_{\hat{f}})^2] &= \mathbb{E}_F \mathbb{E}_{D|\hat{f}}[PD_f^2 - 2PD_f \widehat{PD}_{\hat{f}} + \widehat{PD}_{\hat{f}}^2] \\
 &= PD_f^2 - 2PD_f \mathbb{E}_F \mathbb{E}_{D|\hat{f}}[\widehat{PD}_{\hat{f}}] + \mathbb{E}_F \mathbb{E}_{D|\hat{f}}[\widehat{PD}_{\hat{f}}^2] \\
 &= PD_f^2 - 2PD_f \mathbb{E}_F \mathbb{E}_{D|\hat{f}}[\widehat{PD}_{\hat{f}}] + \mathbb{E}_F \text{Var}_{D|\hat{f}}[\widehat{PD}_{\hat{f}}] + \mathbb{E}_F [\mathbb{E}_{D|\hat{f}}[\widehat{PD}_{\hat{f}}]^2] \\
 &= PD_f^2 - 2PD_f \mathbb{E}_F \mathbb{E}_{D|\hat{f}}[\widehat{PD}_{\hat{f}}] + \mathbb{E}_F \text{Var}_{D|\hat{f}}[\widehat{PD}_{\hat{f}}] + \text{Var}_F \mathbb{E}_{D|\hat{f}}[\widehat{PD}_{\hat{f}}] \\
 &\quad + \mathbb{E}_F [\mathbb{E}_{D|\hat{f}}[\widehat{PD}_{\hat{f}}]^2] \\
 &= (PD_f - \mathbb{E}_F \mathbb{E}_{D|\hat{f}}[\widehat{PD}_{\hat{f}}])^2 + \text{Var}_F \mathbb{E}_{D|\hat{f}}[\widehat{PD}_{\hat{f}}] + \mathbb{E}_F \text{Var}_{D|\hat{f}}[\widehat{PD}_{\hat{f}}].
 \end{aligned}$$

The proof for ALE follows by replacing  $PD_f$  with  $ALE_f$  and  $\widehat{PD}_{\hat{f}}$  with  $\widehat{ALE}_{\hat{f}}$  in the equations above. For this replacement argument, it suffices that all involved quantities are well-defined (Assumption (vi)) and have finite second moments (Assumption (v)), and that  $f$ , and hence  $ALE_f$ , is non-random w.r.t.  $\mathbb{P}_F$ .  $\square$

### A.3 Model Bias of the PD (Eq. (6))

*Proof.* Fix  $x_S$ . Consider the product probability space  $(\hat{f}, X_{\bar{S}}) \sim \mathbb{P}_F \otimes \mathbb{P}_{X_{\bar{S}}}$  (cf. Assumption(i)). By Assumption (ii),  $\hat{f}(x_S, X_{\bar{S}})$  is integrable under  $\mathbb{P}_F \otimes \mathbb{P}_{X_{\bar{S}}}$ , hence  $PD_{\hat{f}}(x_S) = \mathbb{E}_{X_{\bar{S}}}[\hat{f}(x_S, X_{\bar{S}})]$  exists for  $\mathbb{P}_F$ -almost all realizations of  $\hat{f}$  and is integrable w.r.t.  $\mathbb{P}_F$ . Now  $\mathbb{E}_F[PD_{\hat{f}}(x_S)] - PD_f(x_S)$  is equal to

$$\mathbb{E}_F \left[ \mathbb{E}_{X_{\bar{S}}}[\hat{f}(x_S, X_{\bar{S}})] \right] - \mathbb{E}_{X_{\bar{S}}}[f(x_S, X_{\bar{S}})] = \mathbb{E}_{X_{\bar{S}}} \left[ \mathbb{E}_F[\hat{f}(x_S, X_{\bar{S}})] - f(x_S, X_{\bar{S}}) \right].$$

This follows by an application of Fubini's theorem (exchange of integrals) since  $\mathbb{E}_F \mathbb{E}_{X_{\bar{S}}}[\|\hat{f}(x_S, X_{\bar{S}})\|] < \infty$  by Assumption (ii).  $\square$

### A.4 Model Variance of the PD (Eq. (7))

*Proof.* As in §A.3, fix  $x_S$  and suppose Assumptions (i) and (ii) hold. Then, the variance of the theoretical model PD exists and is:

$$\text{Var}_F [PD_{\hat{f}}(x_S)] = \mathbb{E}_F \left[ (\mathbb{E}_{X_{\bar{S}}}[\hat{f}(x_S, X_{\bar{S}})] - \mathbb{E}_F \mathbb{E}_{X_{\bar{S}}}[\hat{f}(x_S, X_{\bar{S}})])^2 \right].$$

Applying Fubini's theorem as  $\mathbb{E}_F \mathbb{E}_{X_{\bar{S}}}[\|\hat{f}(x_S, X_{\bar{S}})\|] < \infty$  by Assumption (ii), we have  $\mathbb{E}_F \mathbb{E}_{X_{\bar{S}}}[\hat{f}(x_S, X_{\bar{S}})] = \mathbb{E}_{X_{\bar{S}}} \mathbb{E}_F[\hat{f}(x_S, X_{\bar{S}})]$ . By linearity of expectations,  $\text{Var}_F [PD_{\hat{f}}(x_S)] = \mathbb{E}_F \left[ (\mathbb{E}_{X_{\bar{S}}}[\hat{f}(x_S, X_{\bar{S}})] - \mathbb{E}_F[\hat{f}(x_S, X_{\bar{S}})])^2 \right]$ . Defining  $U := \hat{f}(x_S, X_{\bar{S}}) - \mathbb{E}_F[\hat{f}(x_S, X_{\bar{S}})]$  and applying Jensen's inequality to  $\phi(t) = t^2$  yields:  $(\mathbb{E}_{X_{\bar{S}}}[U])^2 \leq \mathbb{E}_{X_{\bar{S}}}[U^2]$ . Therefore,  $\text{Var}_F [PD_{\hat{f}}(x_S)] \leq \mathbb{E}_F \mathbb{E}_{X_{\bar{S}}}[U^2]$ . Since  $U^2 \geq 0$ , Tonelli's theorem completes the proof:

$$\text{Var}_F [PD_{\hat{f}}(x_S)] \leq \mathbb{E}_F \mathbb{E}_{X_{\bar{S}}}[U^2] = \mathbb{E}_{X_{\bar{S}}} \mathbb{E}_F[U^2] = \mathbb{E}_{X_{\bar{S}}} \text{Var}_F [\hat{f}(x_S, X_{\bar{S}})]. \quad \square$$

### A.5 Estimation Variance of the PD (Eq. (8))

*Proof.* Fix  $x_S$  and a model  $\hat{f}$ . Suppose Assumption (ii) holds, and consider i.i.d. draws  $D = \{X_{\bar{S}}^{(i)}\}_{i=1}^n$  from  $\mathbb{P}_{X_{\bar{S}}|\hat{f}}$ , conditional on  $\hat{f}$ . Define  $\hat{Y}_S^{(i)} := \hat{f}(x_S, X_{\bar{S}}^{(i)})$ , then by construction the  $\hat{Y}_S^{(i)}$  are i.i.d. conditional on  $\hat{f}$ , and by Assumption (ii), we have  $\mathbb{E}_{X_{\bar{S}}^{(i)}|\hat{f}}[(\hat{Y}_S^{(i)})^2] < \infty$  for  $\mathbb{P}_F$ -almost all  $\hat{f}$ . Thereby

$$\begin{aligned} \text{Var}_{D|\hat{f}}[\widehat{PD}_{\hat{f}}(x_S)] &= \text{Var}_{D|\hat{f}}\left[\frac{1}{n} \sum_{i=1}^n \hat{Y}_S^{(i)}\right] = \frac{1}{n^2} \text{Var}_{D|\hat{f}}\left[\sum_{i=1}^n \hat{Y}_S^{(i)}\right] \\ &= \frac{1}{n^2} \left(\sum_{i=1}^n \text{Var}_{D|\hat{f}}[\hat{Y}_S^{(i)}]\right) = \frac{1}{n^2} \left(n \text{Var}_{D|\hat{f}}[\hat{Y}_S^{(1)}]\right) = \frac{1}{n} \text{Var}_{D|\hat{f}}[\hat{f}(x_S, X_{\bar{S}})], \end{aligned}$$

with  $X_{\bar{S}}$  in the last step being drawn conditional on  $\hat{f}$ , so from  $D | \hat{f}$ . Taking expectation over the training randomness of  $\hat{f}$  gives the proof.  $\square$

### A.6 ALE Estimator Bias w.r.t. Binned Population ALE (§4.2)

*Proof.* Fix  $x_S$ , bins  $\{I_S(k)\}_{k=1}^K$ , and a realization of  $\hat{f}$ . Suppose Assumptions (iii) and (v) hold. Moreover, assume  $D = \{X^{(i)}\}_{i=1}^n$  (used for estimation) are i.i.d. draws from  $\mathbb{P}_X$ , independent of  $\hat{f}$ , and assume  $n_S(k) > 0$  for all bins  $k \leq k_S(x_S)$ . Let  $B = (B^{(1)}, \dots, B^{(n)})$  be the bin assignments of the samples, where  $B^{(i)} = k_S(X_S^{(i)})$ . Then, conditional on the *full* assignment vector  $B$ , i.e., on the product event  $\bigcap_{i=1}^n \{X_S^{(i)} \in I_S(B^{(i)})\}$ , the samples remain independent; in particular, for each  $k$  the subcollection  $\{X_S^{(i)} : B^{(i)} = k\}$  is i.i.d. with  $X_{\bar{S}}^{(i)} \sim \mathbb{P}_{X_{\bar{S}}|X_S \in I_S(k)}$ . Therefore, using the law of total expectation and  $D \perp \hat{f}$ , we obtain

$$\begin{aligned} \mathbb{E}_{D|\hat{f}}\left[\widehat{ALE}_{\hat{f}}(x_S)\right] &= \mathbb{E}_B \mathbb{E}_{D|B} \left[ \sum_{k=1}^{k_S(x_S)} \frac{1}{n_S(k)} \sum_{i: X_S^{(i)} \in I_S(k)} \Delta_{\hat{f}}(k, X_{\bar{S}}^{(i)}) \right] \\ &= \mathbb{E}_B \left[ \sum_{k=1}^{k_S(x_S)} \frac{1}{n_S(k)} \sum_{i: X_S^{(i)} \in I_S(k)} \mathbb{E}_{D|B} [\Delta_{\hat{f}}(k, X_{\bar{S}}^{(i)})] \right] \\ &= \mathbb{E}_B \left[ \sum_{k=1}^{k_S(x_S)} \mathbb{E}_{X_{\bar{S}}|X_S \in I_S(k)} [\Delta_{\hat{f}}(k, X_{\bar{S}})] \right] = \mathbb{E}_B[\widehat{ALE}_{\hat{f}}^K(x_S)] = \widehat{ALE}_{\hat{f}}^K(x_S). \end{aligned}$$

Thus,  $\widehat{ALE}_{\hat{f}}$  is unbiased for  $\widehat{ALE}_{\hat{f}}^K : \mathbb{E}_{D|\hat{f}}[\widehat{ALE}_{\hat{f}}(x_S)] - \widehat{ALE}_{\hat{f}}^K(x_S) = 0$ .  $\square$

### A.7 Model Bias of the ALE (§4.2)

*Proof.* Fix  $x_S$  and let  $\hat{f} \sim \mathbb{P}_F$ . Suppose Assumptions (i), (iii), (iv), and (v) hold, so  $(X_S, X_{\bar{S}}) \sim \mathbb{P}_X$  is an independent population draw, i.e.,  $(X_S, X_{\bar{S}}) \perp \hat{f}$ , and

$\widetilde{ALE}_{\hat{f}}(x_S)$  and  $\widetilde{ALE}_f(x_S)$  exist by Assumption (vi). For  $K \in \mathbb{N}$ , define  $g_K(\hat{f}) := \sum_{k=1}^{k_S^K(x_S)} \mathbb{E}_{X_{\bar{S}}|X_S \in I_S^K(k)}[\Delta_{\hat{f},S}^K(k, X_{\bar{S}})]$ , so that  $\widetilde{ALE}_{\hat{f}}(x_S) = \lim_{K \rightarrow \infty} g_K(\hat{f})$  by definition. Then,

$$\begin{aligned} \mathbb{E}_F[\widetilde{ALE}_{\hat{f}}(x_S)] &= \int_{\mathcal{F}} \lim_{K \rightarrow \infty} g_K(\hat{f}) \, d\mathbb{P}_F(\hat{f}) = \lim_{K \rightarrow \infty} \int_{\mathcal{F}} g_K(\hat{f}) \, d\mathbb{P}_F(\hat{f}) \\ &= \lim_{K \rightarrow \infty} \sum_{k=1}^{k_S^K(x_S)} \int_{\mathcal{F}} \mathbb{E}_{X_{\bar{S}}|X_S \in I_S^K(k)}[\Delta_{\hat{f},S}^K(k, X_{\bar{S}})] \, d\mathbb{P}_F(\hat{f}) \\ &= \lim_{K \rightarrow \infty} \sum_{k=1}^{k_S^K(x_S)} \mathbb{E}_{X_{\bar{S}}|X_S \in I_S^K(k)}[\mathbb{E}_F[\Delta_{\hat{f},S}^K(k, X_{\bar{S}})]] . \end{aligned}$$

The second equality follows from the Dominated Convergence Theorem. Indeed,  $g_K(\hat{f}) \rightarrow \widetilde{ALE}_{\hat{f}}(x_S)$  pointwise in  $\hat{f}$  by definition, and for every  $K$ ,

$$\begin{aligned} |g_K(\hat{f})| &\leq \sum_{k=1}^{k_S^K(x_S)} \mathbb{E}_{X_{\bar{S}}|X_S \in I_S^K(k)}[|\Delta_{\hat{f},S}^K(k, X_{\bar{S}})|] \leq \sum_{k=1}^{k_S^K(x_S)} \operatorname{ess\,sup}_{\mathbf{x}_{\bar{S}}} |\Delta_{\hat{f},S}^K(k, \mathbf{x}_{\bar{S}})| \\ &\leq \operatorname{ess\,sup}_{\mathbf{x}_{\bar{S}}} \sum_{k=1}^{k_S^K(x_S)} |\hat{f}(z_{k,S}^K, \mathbf{x}_{\bar{S}}) - \hat{f}(z_{k-1,S}^K, \mathbf{x}_{\bar{S}})| \\ &\leq \operatorname{ess\,sup}_{\mathbf{x}_{\bar{S}}} \operatorname{TV}(t \mapsto \hat{f}(t, \mathbf{x}_{\bar{S}})) \leq V(\hat{f}), \end{aligned}$$

where  $V(\hat{f})$  is the integrable bound from Assumption (iv). The last equality above follows from Fubini's theorem, using Assumption (v) (integrability) for  $\mathbb{P}_{X_{\bar{S}}|X_S \in I_S^K(k), \hat{f}} = \mathbb{P}_{X_{\bar{S}}|X_S \in I_S^K(k)}$  since  $(X_S, X_{\bar{S}}) \perp \hat{f}$ . By linearity of expectation,

$$\begin{aligned} \mathbb{E}_F[\widetilde{ALE}_{\hat{f}}(x_S)] - \widetilde{ALE}_f(x_S) &= \\ \lim_{K \rightarrow \infty} \sum_{k=1}^{k_S^K(x_S)} \mathbb{E}_{X_{\bar{S}}|X_S \in I_S^K(k)}[\mathbb{E}_F[\Delta_{\hat{f},S}^K(k, X_{\bar{S}})] - \Delta_{f,S}^K(k, X_{\bar{S}})] . \end{aligned}$$

Thus, this bias term vanishes if the finite differences of  $\hat{f}$  are unbiased w.r.t. those of  $f$ . One sufficient condition is that  $\hat{f}$  is a pointwise unbiased estimator of  $f$ .  $\square$

## A.8 Model Variance of the ALE (Eq. (11))

*Proof.* Fix  $x_S$ , let  $\hat{f} \sim \mathbb{P}_F$ , and suppose Assumptions (i), (iii), and (v) hold, so that as in §A.7, for each bin index  $k$ , all expectations w.r.t.  $\mathbb{P}_{X_{\bar{S}}|\mathcal{I}_k}$  are independent of  $\hat{f}$ . For readability, we abbreviate the event  $\{X_S \in I_S(k)\}$  by  $\mathcal{I}_k$ . Then:

$$\begin{aligned}
\text{Var}_F \left[ \widetilde{ALE}_{\hat{f}}^K(x_S) \right] &= \text{Var}_F \left( \sum_{k=1}^{k_S(x_S)} \mathbb{E}_{X_{\bar{S}}|\mathcal{I}_k} [\Delta_{\hat{f}}(k, X_{\bar{S}})] \right) \\
&= \mathbb{E}_F \left[ \left( \sum_{k=1}^{k_S(x_S)} \mathbb{E}_{X_{\bar{S}}|\mathcal{I}_k} [\Delta_{\hat{f}}(k, X_{\bar{S}})] - \mathbb{E}_F \left[ \sum_{k=1}^{k_S(x_S)} \mathbb{E}_{X_{\bar{S}}|\mathcal{I}_k} [\Delta_{\hat{f}}(k, X_{\bar{S}})] \right] \right)^2 \right] \\
&= \mathbb{E}_F \left[ \left( \sum_{k=1}^{k_S(x_S)} \mathbb{E}_{X_{\bar{S}}|\mathcal{I}_k} \left[ \Delta_{\hat{f}}(k, X_{\bar{S}}) - \mathbb{E}_F [\Delta_{\hat{f}}(k, X_{\bar{S}})] \right] \right)^2 \right].
\end{aligned}$$

The last line follows from the linearity of expectations and exchanging  $\mathbb{E}_F$  and  $\mathbb{E}_{X_{\bar{S}}|\mathcal{I}_k}$  by an application of Fubini's theorem. Indeed, using Assumption (v) for  $\hat{f} \perp (X_S, X_{\bar{S}})$  ensures that the resulting joint integrand is integrable. Define  $U_k := \mathbb{E}_{X_{\bar{S}}|\mathcal{I}_k} [\Delta_{\hat{f}}(k, X_{\bar{S}}) - \mathbb{E}_F [\Delta_{\hat{f}}(k, X_{\bar{S}})]]$ , and let  $\mathbf{U} = (U_1, \dots, U_{k_S(x_S)})^\top$ . By the Cauchy-Schwarz inequality,  $(\sum_{k=1}^{k_S(x_S)} U_k)^2 = \langle \mathbf{1}, \mathbf{U} \rangle^2 \leq \|\mathbf{1}\|^2 \|\mathbf{U}\|^2 = k_S(x_S) \sum_{k=1}^{k_S(x_S)} U_k^2$ . Moreover,  $\mathbb{E}_F [k_S(x_S) \sum_{k=1}^{k_S(x_S)} U_k^2] = k_S(x_S) \sum_{k=1}^{k_S(x_S)} \mathbb{E}_F [U_k^2]$  by linearity of expectation. By Assumption (v), applying Jensen's inequality to  $\varphi(t) = t^2$ , we obtain  $U_k^2 \leq \mathbb{E}_{X_{\bar{S}}|\mathcal{I}_k} [(\Delta_{\hat{f}}(k, X_{\bar{S}}) - \mathbb{E}_F [\Delta_{\hat{f}}(k, X_{\bar{S}})])^2]$ . Putting everything together and applying Tonelli's theorem (the integrand  $U_k^2$  is non-negative) gives the proof:

$$\begin{aligned}
\text{Var}_F \left[ \widetilde{ALE}_{\hat{f}}^K(x_S) \right] &\leq k_S(x_S) \sum_{k=1}^{k_S(x_S)} \mathbb{E}_F \mathbb{E}_{X_{\bar{S}}|\mathcal{I}_k} \left[ \left( \Delta_{\hat{f}}(k, X_{\bar{S}}) - \mathbb{E}_F [\Delta_{\hat{f}}(k, X_{\bar{S}})] \right)^2 \right] \\
&= k_S(x_S) \sum_{k=1}^{k_S(x_S)} \mathbb{E}_{X_{\bar{S}}|\mathcal{I}_k} \mathbb{E}_F \left[ \left( \Delta_{\hat{f}}(k, X_{\bar{S}}) - \mathbb{E}_F [\Delta_{\hat{f}}(k, X_{\bar{S}})] \right)^2 \right] \\
&= k_S(x_S) \sum_{k=1}^{k_S(x_S)} \mathbb{E}_{X_{\bar{S}}|\mathcal{I}_k} \text{Var}_F [\Delta_{\hat{f}}(k, X_{\bar{S}})]. \quad \square
\end{aligned}$$

### A.9 Estimation Variance of the ALE (Eq. (12))

*Proof.* Fix  $x_S$  and bins  $I_S(k)$ , suppose Assumptions (iii), (v) and (vi) hold, i.p. with  $D = \{X^{(i)}\}_{i=1}^n$  being i.i.d. draws from  $\mathbb{P}_{X|f}$ , conditional on  $\hat{f}$ , and assume  $n_S(k) > 0 \forall k$ . For any fixed  $k$ , the variance of the finite differences  $\sigma_k^2(\hat{f}) := \text{Var}_{X_{\bar{S}}|X_S \in I_S(k), \hat{f}} [\Delta_{\hat{f}}(k, X_{\bar{S}})]$  is finite by Assumption (v):  $\sigma_k^2(\hat{f}) < \infty$ . Now, for each  $k$ , conditional on a model  $\hat{f}$  and on the full bin assignment vector  $B$  of all samples, the variables  $\{\Delta_{\hat{f}}(k, X_{\bar{S}}^{(i)}) : B^{(i)} = k\}$  (all those falling into  $I_S(k)$ ) are i.i.d. with variance  $\sigma_k^2(\hat{f})$ . Since also  $n_S(k)$  and the events  $\{X_S^{(i)} \in I_S(k)\}$  are fixed conditional on  $B$  and  $\hat{f}$  (similar to §A.6), this gives

us  $\text{Var}_{D|\hat{f},B}[\hat{\mu}_k(\hat{f})] = \sigma_k^2(\hat{f})/n_S(k)$ , where we define the unaccumulated value of the  $k$ -th bin as  $\hat{\mu}_k(\hat{f}) := \frac{1}{n_S(k)} \sum_{i: X_S^{(i)} \in I_S(k)} \Delta_{\hat{f}}(k, X_S^{(i)})$ . Moreover, conditional on  $B$  and  $\hat{f}$ , different bins use disjoint subsets of the i.i.d. sample, hence  $\text{Cov}_{D|\hat{f},B}[\hat{\mu}_k(\hat{f}), \hat{\mu}_\ell(\hat{f})] = 0$  for  $k \neq \ell$ . Altogether we get:

$$\begin{aligned} \mathbb{E}_F \mathbb{E}_{B|\hat{f}} \text{Var}_{D|\hat{f},B} \left[ \widehat{ALE}_{\hat{f}}(x_S) \right] &= \mathbb{E}_F \mathbb{E}_{B|\hat{f}} \text{Var}_{D|\hat{f},B} \left[ \sum_{k \leq k_S(x_S)} \hat{\mu}_k(\hat{f}) \right] \\ &= \sum_{k \leq k_S(x_S)} \mathbb{E}_F \mathbb{E}_{B|\hat{f}} \text{Var}_{D|\hat{f},B} [\hat{\mu}_k(\hat{f})] = \sum_{k \leq k_S(x_S)} \mathbb{E}_F \mathbb{E}_{B|\hat{f}} \left[ \frac{1}{n_S(k)} \sigma_k^2(\hat{f}) \right]. \quad \square \end{aligned}$$

## B Simulation Details & Results

### B.1 Models, Hyperparameters, and Model Performances

The XGBoost implementation from *xgboost* [4], and the GAM implementation from *pyGAM* [22] were used. For the GAM, we considered the number of basis functions ( $\in [5, 50]$ ) and the penalization control parameter ( $\in [0.001, 1000]$ , log-uniform) as tuning parameters. For XGBoost, we used the parameter spaces from [21] (confined to trees as base learners).

Hyperparameter configurations for the overfitting models (OF) were carefully hand-picked to achieve strong performance on the training data while performing relatively poorly on holdout data. The optimal hyperparameters (OT) were selected by tuning the models on a separate data sample of size  $n$  (1250 or 10000) for 200 trials using a Tree-structured Parzen Estimator (TPE) [2] with MSE on separate holdout data (10000 samples for reliable performance estimates) as minimization objective. For both OF and OT models, the final selected hyperparameter configurations can be found on Github ([link](#)).

We evaluate model performance across all repetitions on both the training and test data, with 10000 test samples to obtain reliable performance estimates. As intended, overfitting models show better training performance than the optimally tuned models, but underperform on test data and exhibit higher variance in their generalization performance. A linear regression model is used as a baseline and is outperformed by all OT models. These performance metrics can be found on GitHub ([link](#)).

### B.2 Further Results: Bias-Variance-Analysis

Table 6: Results for PD on *Friedman1* averaged over 100 grid points. Bold numbers indicate the minimum per metric-feature-model-size-combination.

		Feature Metric	MSE	$x_1$ Bias	Var	MSE	$x_3$ Bias	Var	MSE	$x_5$ Bias	Var
$n = 1250$	GAM_OF	train	0.1184	0.0720	0.1173	0.1285	<b>0.0639</b>	0.1289	0.1210	<b>0.0631</b>	0.1212
		val	0.1968	0.0929	0.1949	0.2084	0.0907	0.2073	0.2302	0.0955	0.2289
		CV	<b>0.1062</b>	<b>0.0697</b>	<b>0.1049</b>	<b>0.1094</b>	0.0650	<b>0.1090</b>	<b>0.1057</b>	0.0652	<b>0.1051</b>
	GAM_OT	train	0.0166	0.0190	0.0168	0.0146	0.0238	0.0145	0.0145	<b>0.0166</b>	0.0147
		val	0.0264	0.0266	0.0266	0.0187	0.0236	0.0188	0.0199	0.0221	0.0201
		CV	<b>0.0165</b>	<b>0.0182</b>	<b>0.0167</b>	<b>0.0144</b>	<b>0.0236</b>	<b>0.0143</b>	<b>0.0143</b>	0.0166	<b>0.0146</b>
	XGB_OF	train	0.1361	<b>0.2297</b>	0.0862	<b>0.4853</b>	<b>0.6748</b>	0.0310	0.1142	<b>0.2767</b>	0.0390
		val	0.1915	0.2885	0.1120	0.6402	0.7744	0.0419	0.1718	0.3097	0.0786
		CV	<b>0.1196</b>	0.2742	<b>0.0460</b>	0.5429	0.7258	<b>0.0167</b>	<b>0.1055</b>	0.2853	<b>0.0249</b>
XGB_OT	train	<b>0.0327</b>	<b>0.1081</b>	0.0217	<b>0.0393</b>	<b>0.1511</b>	0.0170	<b>0.0208</b>	<b>0.0854</b>	0.0140	
	val	0.0416	0.1206	0.0280	0.0509	0.1752	0.0209	0.0245	0.0925	0.0165	
	CV	0.0334	0.1227	<b>0.0190</b>	0.0439	0.1718	<b>0.0149</b>	0.0209	0.0941	<b>0.0125</b>	
$n = 10000$	GAM_OF	train	<b>0.0094</b>	0.0178	<b>0.0094</b>	<b>0.0086</b>	<b>0.0173</b>	<b>0.0086</b>	<b>0.0096</b>	0.0192	<b>0.0096</b>
		val	0.0137	0.0212	0.0137	0.0117	0.0211	0.0117	0.0129	0.0235	0.0128
		CV	0.0095	<b>0.0178</b>	0.0095	0.0087	0.0173	0.0086	0.0097	<b>0.0189</b>	0.0096
	GAM_OT	train	0.0005	0.0082	0.0005	<b>0.0004</b>	0.0024	<b>0.0004</b>	<b>0.0004</b>	<b>0.0035</b>	<b>0.0004</b>
		val	0.0013	<b>0.0076</b>	0.0013	0.0005	<b>0.0021</b>	0.0005	0.0005	0.0049	0.0005
		CV	<b>0.0005</b>	0.0082	<b>0.0005</b>	0.0004	0.0024	0.0004	0.0004	0.0036	0.0004
	XGB_OF	train	<b>0.0232</b>	<b>0.1194</b>	0.0092	<b>0.0675</b>	<b>0.2523</b>	0.0040	<b>0.0302</b>	<b>0.1594</b>	0.0049
		val	0.0326	0.1370	0.0143	0.0924	0.2949	0.0057	0.0386	0.1776	0.0073
		CV	0.0235	0.1314	<b>0.0065</b>	0.0860	0.2886	<b>0.0028</b>	0.0344	0.1753	<b>0.0038</b>
XGB_OT	train	0.0060	<b>0.0266</b>	0.0055	0.0060	<b>0.0374</b>	0.0047	0.0044	<b>0.0274</b>	0.0038	
	val	0.0078	0.0318	0.0070	0.0073	0.0428	0.0057	0.0055	0.0327	0.0046	
	CV	<b>0.0052</b>	0.0293	<b>0.0045</b>	<b>0.0056</b>	0.0427	<b>0.0039</b>	<b>0.0041</b>	0.0310	<b>0.0033</b>	

Table 7: Results for ALE on *Friedman1* averaged over 100 grid points. Bold numbers indicate the minimum per metric-feature-model-size-combination.

		Feature Metric	MSE	$x_1$ Bias	Var	MSE	$x_3$ Bias	Var	MSE	$x_5$ Bias	Var
$n = 1250$	GAM_OF	train	<b>0.1280</b>	<b>0.0809</b>	<b>0.1258</b>	<b>0.1290</b>	<b>0.0629</b>	<b>0.1295</b>	0.1246	<b>0.0642</b>	0.1248
		val	0.4060	0.1738	0.3892	0.4199	0.2139	0.3875	0.4212	0.1265	0.4196
		CV	0.1745	0.1855	0.1451	0.1497	0.1479	0.1324	<b>0.1212</b>	0.0951	<b>0.1162</b>
	GAM_OT	train	<b>0.0206</b>	<b>0.0336</b>	0.0201	<b>0.0146</b>	<b>0.0235</b>	0.0145	<b>0.0144</b>	<b>0.0165</b>	0.0146
		val	0.0795	0.1668	0.0535	0.0403	0.1219	0.0263	0.0316	0.1086	0.0205
		CV	0.0400	0.1449	<b>0.0196</b>	0.0273	0.1159	<b>0.0144</b>	0.0257	0.1147	<b>0.0130</b>
	XGB_OF	train	3.6571	1.6329	1.0248	1.2235	0.8780	0.4683	2.6986	1.4763	0.5371
		val	4.8262	0.5670	4.6600	1.5224	<b>0.7511</b>	0.9914	1.9319	0.4747	1.7654
		CV	<b>0.8781</b>	<b>0.4926</b>	<b>0.6573</b>	<b>0.7944</b>	0.7932	<b>0.1710</b>	<b>0.5237</b>	<b>0.4235</b>	<b>0.3562</b>
XGB_OT	train	<b>0.0591</b>	<b>0.1629</b>	0.0337	<b>0.0344</b>	<b>0.0961</b>	0.0260	<b>0.0482</b>	<b>0.1701</b>	0.0199	
	val	0.1411	0.2250	0.0937	0.1314	0.2818	0.0538	0.0770	0.1795	0.0463	
	CV	0.0878	0.2428	<b>0.0299</b>	0.0920	0.2690	<b>0.0203</b>	0.0563	0.1989	<b>0.0173</b>	
$n = 10000$	GAM_OF	train	<b>0.0107</b>	0.0272	<b>0.0103</b>	<b>0.0087</b>	0.0171	<b>0.0087</b>	<b>0.0096</b>	0.0191	<b>0.0096</b>
		val	0.0177	0.0312	0.0173	0.0127	0.0214	0.0127	0.0135	0.0237	0.0133
		CV	0.0107	<b>0.0267</b>	0.0103	0.0088	<b>0.0171</b>	0.0088	0.0097	<b>0.0189</b>	0.0097
	GAM_OT	train	<b>0.0016</b>	0.0239	<b>0.0011</b>	0.0004	0.0023	0.0004	<b>0.0004</b>	<b>0.0036</b>	<b>0.0004</b>
		val	0.0036	<b>0.0233</b>	0.0031	0.0005	<b>0.0023</b>	0.0005	0.0005	0.0048	0.0005
		CV	0.0016	0.0239	0.0011	<b>0.0004</b>	0.0024	<b>0.0004</b>	0.0004	0.0036	0.0004
	XGB_OF	train	0.6796	0.8044	0.0336	0.4915	0.6802	0.0299	0.8473	0.9057	0.0279
		val	0.2098	0.1518	0.1932	0.1711	0.3057	0.0803	0.1157	<b>0.1788</b>	0.0866
		CV	<b>0.0485</b>	<b>0.1308</b>	<b>0.0324</b>	<b>0.1091</b>	<b>0.3024</b>	<b>0.0183</b>	<b>0.0499</b>	0.1821	<b>0.0173</b>
XGB_OT	train	0.0070	<b>0.0252</b>	0.0066	<b>0.0055</b>	<b>0.0209</b>	0.0052	0.0045	<b>0.0164</b>	0.0044	
	val	0.0166	0.0392	0.0155	0.0112	0.0483	0.0091	0.0075	0.0291	0.0069	
	CV	<b>0.0064</b>	0.0276	<b>0.0058</b>	0.0062	0.0436	<b>0.0044</b>	<b>0.0045</b>	0.0307	<b>0.0037</b>	

Table 8: Results for PD on *Feynman I.29.16* averaged over 100 grid points. Bold numbers indicate the minimum per metric-feature-model-size-combination.

		Feature Metric	MSE	$x_1$ Bias	Var	MSE	$\theta_1$ Bias	Var	MSE	$d_1$ Bias	Var
$n = 1250$	GAM_OF	train	0.2916	0.1357	0.2826	0.0660	0.0482	0.0659	0.0693	0.0497	0.0692
		val	0.4493	0.1492	0.4417	0.0988	0.0617	0.0982	0.1011	0.0528	0.1017
		CV	<b>0.1577</b>	<b>0.0749</b>	<b>0.1574</b>	<b>0.0611</b>	<b>0.0458</b>	<b>0.0610</b>	<b>0.0650</b>	<b>0.0485</b>	<b>0.0648</b>
	GAM_OT	train	0.0318	0.0358	0.0316	0.0199	0.0281	0.0197	0.0179	0.0194	0.0182
		val	0.0430	0.0370	0.0431	0.0255	0.0310	0.0254	0.0215	0.0224	0.0217
		CV	<b>0.0299</b>	<b>0.0344</b>	<b>0.0297</b>	<b>0.0186</b>	<b>0.0273</b>	<b>0.0185</b>	<b>0.0170</b>	<b>0.0193</b>	<b>0.0172</b>
	XGB_OF	train	0.0681	0.0623	0.0664	0.0032	<b>0.0209</b>	0.0029	0.0030	0.0105	0.0030
		val	0.0878	0.0715	0.0855	0.0049	0.0245	0.0044	0.0039	0.0178	0.0037
		CV	<b>0.0429</b>	<b>0.0408</b>	<b>0.0426</b>	<b>0.0021</b>	0.0217	<b>0.0016</b>	<b>0.0014</b>	<b>0.0044</b>	<b>0.0014</b>
XGB_OT	train	0.0316	<b>0.0746</b>	0.0270	0.0095	0.0229	0.0093	0.0074	0.0138	0.0074	
	val	0.0404	0.0813	0.0349	0.0117	0.0227	0.0116	0.0083	0.0162	0.0083	
	CV	<b>0.0297</b>	0.0865	<b>0.0230</b>	<b>0.0079</b>	<b>0.0221</b>	<b>0.0077</b>	<b>0.0063</b>	<b>0.0129</b>	<b>0.0064</b>	
$n = 10000$	GAM_OF	train	0.0146	0.0221	0.0146	0.0072	0.0214	0.0070	0.0071	0.0160	0.0071
		val	0.0192	0.0253	0.0192	0.0090	0.0217	0.0088	0.0090	0.0184	0.0089
		CV	<b>0.0142</b>	<b>0.0219</b>	<b>0.0142</b>	<b>0.0070</b>	<b>0.0212</b>	<b>0.0068</b>	<b>0.0069</b>	<b>0.0156</b>	<b>0.0068</b>
	GAM_OT	train	0.0061	0.0135	0.0061	0.0036	0.0179	0.0034	0.0033	0.0123	0.0033
		val	0.0075	0.0166	0.0075	0.0040	<b>0.0156</b>	0.0039	0.0039	0.0134	0.0039
		CV	<b>0.0058</b>	<b>0.0134</b>	<b>0.0058</b>	<b>0.0034</b>	0.0178	<b>0.0032</b>	<b>0.0032</b>	<b>0.0121</b>	<b>0.0032</b>
	XGB_OF	train	0.0103	0.0198	0.0103	0.0014	0.0293	0.0006	0.0007	0.0080	0.0006
		val	0.0124	0.0207	0.0124	0.0017	0.0293	0.0008	0.0007	0.0078	0.0007
		CV	<b>0.0066</b>	<b>0.0156</b>	<b>0.0065</b>	<b>0.0012</b>	<b>0.0290</b>	<b>0.0004</b>	<b>0.0004</b>	<b>0.0069</b>	<b>0.0004</b>
XGB_OT	train	0.0057	<b>0.0181</b>	0.0056	0.0028	0.0203	0.0024	0.0023	0.0098	0.0023	
	val	0.0072	0.0204	0.0070	0.0033	<b>0.0202</b>	0.0030	0.0026	0.0106	0.0025	
	CV	<b>0.0045</b>	0.0185	<b>0.0043</b>	<b>0.0024</b>	0.0204	<b>0.0020</b>	<b>0.0018</b>	<b>0.0093</b>	<b>0.0018</b>	

Table 9: Results for ALE on *Feynman I.29.16* averaged over 100 grid points. Bold numbers indicate the minimum per metric-feature-model-size-combination.

		Feature Metric	MSE	$x_1$ Bias	Var	MSE	$\theta_1$ Bias	Var	MSE	$d_1$ Bias	Var
$n = 1250$	GAM_OF	train	0.3122	<b>0.1226</b>	0.3075	<b>0.0701</b>	0.0591	<b>0.0689</b>	<b>0.0738</b>	<b>0.0506</b>	<b>0.0737</b>
		val	0.7270	0.2335	0.6956	0.2011	0.0703	0.2029	0.1729	0.0797	0.1723
		CV	<b>0.2393</b>	0.2227	<b>0.1963</b>	0.0712	<b>0.0503</b>	0.0711	0.0786	0.0556	0.0781
	GAM_OT	train	<b>0.0337</b>	<b>0.0405</b>	0.0332	0.0214	<b>0.0400</b>	0.0205	0.0179	0.0195	0.0181
		val	0.0827	0.1494	0.0625	0.0322	0.0437	0.0314	0.0220	0.0230	0.0222
		CV	0.0604	0.1697	<b>0.0327</b>	<b>0.0185</b>	0.0409	<b>0.0174</b>	<b>0.0146</b>	<b>0.0183</b>	<b>0.0148</b>
	XGB_OF	train	0.5272	0.3080	0.4473	0.1359	0.0539	0.1376	0.1118	0.0677	0.1109
		val	1.8846	<b>0.2021</b>	1.9073	0.1266	0.0616	0.1270	0.0653	<b>0.0428</b>	0.0656
		CV	<b>0.3804</b>	0.2820	<b>0.3113</b>	<b>0.0381</b>	<b>0.0520</b>	<b>0.0366</b>	<b>0.0338</b>	0.0502	<b>0.0323</b>
XGB_OT	train	<b>0.0362</b>	<b>0.0421</b>	0.0356	0.0186	0.0379	0.0177	0.0129	0.0176	0.0130	
	val	0.1037	0.1760	0.0752	0.0318	<b>0.0277</b>	0.0321	0.0189	0.0240	0.0189	
	CV	0.0790	0.2141	<b>0.0344</b>	<b>0.0120</b>	0.0397	<b>0.0108</b>	<b>0.0076</b>	<b>0.0146</b>	<b>0.0076</b>	
$n = 10000$	GAM_OF	train	0.0149	0.0257	0.0147	0.0079	0.0304	0.0072	0.0072	0.0162	0.0072
		val	0.0219	0.0294	0.0218	0.0114	0.0308	0.0108	0.0096	0.0190	0.0096
		CV	<b>0.0148</b>	<b>0.0255</b>	<b>0.0147</b>	<b>0.0077</b>	<b>0.0303</b>	<b>0.0070</b>	<b>0.0070</b>	<b>0.0156</b>	<b>0.0070</b>
	GAM_OT	train	0.0063	0.0191	0.0062	0.0041	0.0279	0.0035	0.0033	0.0123	0.0033
		val	0.0081	0.0230	0.0078	0.0052	<b>0.0268</b>	0.0046	0.0040	0.0134	0.0039
		CV	<b>0.0061</b>	<b>0.0191</b>	<b>0.0059</b>	<b>0.0040</b>	0.0278	<b>0.0033</b>	<b>0.0032</b>	<b>0.0120</b>	<b>0.0032</b>
	XGB_OF	train	0.0470	0.0386	0.0471	0.0199	0.0541	0.0175	0.0105	0.0331	0.0098
		val	0.2569	0.0855	0.2582	0.0197	0.0568	0.0171	0.0129	0.0196	0.0129
		CV	<b>0.0358</b>	<b>0.0354</b>	<b>0.0357</b>	<b>0.0059</b>	<b>0.0459</b>	<b>0.0039</b>	<b>0.0037</b>	<b>0.0178</b>	<b>0.0035</b>
XGB_OT	train	0.0069	<b>0.0154</b>	0.0069	0.0045	<b>0.0241</b>	0.0041	0.0029	0.0116	0.0029	
	val	0.0154	0.0212	0.0154	0.0087	0.0293	0.0081	0.0043	0.0132	0.0043	
	CV	<b>0.0058</b>	0.0256	<b>0.0054</b>	<b>0.0043</b>	0.0293	<b>0.0035</b>	<b>0.0022</b>	<b>0.0098</b>	<b>0.0022</b>	

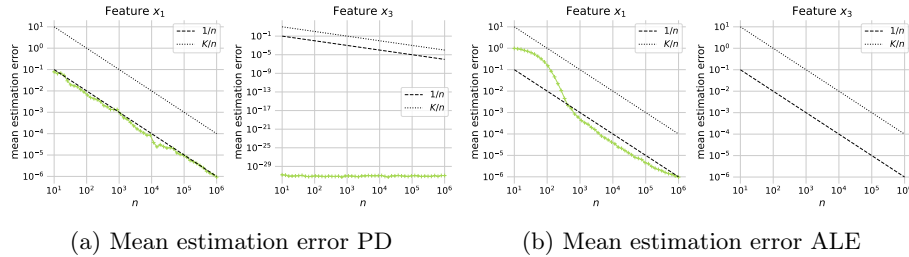
Table 10: Decomposition results of total variance  $\text{Var}_{\text{Tot}}$  into model  $\text{Var}_{\text{Mod}}$  and estimation variance  $\text{Var}_{\text{Est}}$  on *SimpleNormalCorrelated* averaged over 100 grid points. Bold numbers indicate estimation strategy with minimal variance.

		Feature Metric	$x_1$			$x_2$			$x_3$		
			$\text{Var}_{\text{Tot}}$	$\text{Var}_{\text{Mod}}$	$\text{Var}_{\text{Est}}$	$\text{Var}_{\text{Tot}}$	$\text{Var}_{\text{Mod}}$	$\text{Var}_{\text{Est}}$	$\text{Var}_{\text{Tot}}$	$\text{Var}_{\text{Mod}}$	$\text{Var}_{\text{Est}}$
PD	XGB_OF	train	0.0817	0.0813	0.0004	0.2263	0.2259	0.0004	0.0010	0.0009	0.0001
		val	0.0857	0.0837	0.0020	0.2416	0.2395	0.0021	0.0014	0.0011	0.0003
		CV	<b>0.0505</b>	<b>0.0501</b>	<b>0.0004</b>	<b>0.1291</b>	<b>0.1287</b>	<b>0.0004</b>	<b>0.0007</b>	<b>0.0006</b>	<b>0.0001</b>
XGB_OT	train	0.0113	0.0112	<b>0.0001</b>	0.0141	0.0141	<b>0.0001</b>	0.0014	0.0014	0.0000	
	val	0.0123	0.0119	0.0004	0.0155	0.0151	0.0004	0.0019	0.0019	0.0000	
	CV	<b>0.0090</b>	<b>0.0089</b>	0.0001	<b>0.0104</b>	<b>0.0103</b>	0.0001	<b>0.0013</b>	<b>0.0013</b>	<b>0.0000</b>	
ALE	XGB_OF	train	<b>0.1012</b>	<b>0.0161</b>	<b>0.0851</b>	0.1011	0.0249	<b>0.0762</b>	0.0741	0.0636	<b>0.0105</b>
		val	0.5281	0.0359	0.4923	0.6017	0.1743	0.4275	0.0864	0.0424	0.0439
		CV	0.1520	0.0620	0.0900	<b>0.0994</b>	<b>0.0110</b>	0.0884	<b>0.0121</b>	<b>0.0003</b>	0.0118
XGB_OT	train	0.0088	0.0077	<b>0.0011</b>	0.0119	0.0107	<b>0.0011</b>	0.0066	0.0062	<b>0.0005</b>	
	val	0.0263	0.0124	0.0140	0.0275	0.0089	0.0186	0.0033	<b>0.0003</b>	0.0029	
	CV	<b>0.0077</b>	<b>0.0049</b>	0.0029	<b>0.0103</b>	<b>0.0065</b>	0.0038	<b>0.0020</b>	0.0014	0.0007	

Table 11: Decomposition results of total variance  $\text{Var}_{\text{Tot}}$  into model  $\text{Var}_{\text{Mod}}$  and estimation variance  $\text{Var}_{\text{Est}}$  on *Feynman I.29.16* averaged over 100 grid points. Bold numbers indicate estimation strategy with minimal variance.

		Feature Metric	$x_1$			$\theta_1$			$d_1$		
			$\text{Var}_{\text{Tot}}$	$\text{Var}_{\text{Mod}}$	$\text{Var}_{\text{Est}}$	$\text{Var}_{\text{Tot}}$	$\text{Var}_{\text{Mod}}$	$\text{Var}_{\text{Est}}$	$\text{Var}_{\text{Tot}}$	$\text{Var}_{\text{Mod}}$	$\text{Var}_{\text{Est}}$
PD	XGB_OF	train	0.0664	0.0652	0.0013	0.0029	0.0027	0.0002	0.0030	0.0029	0.0002
		val	0.0855	0.0794	0.0061	0.0044	0.0035	0.0009	0.0037	0.0029	0.0008
		CV	<b>0.0426</b>	<b>0.0414</b>	<b>0.0012</b>	<b>0.0016</b>	<b>0.0015</b>	<b>0.0002</b>	<b>0.0014</b>	<b>0.0013</b>	<b>0.0001</b>
XGB_OT	train	0.0270	0.0266	<b>0.0004</b>	0.0093	0.0091	0.0002	0.0074	0.0074	0.0000	
	val	0.0349	0.0334	0.0015	0.0116	0.0108	0.0007	0.0083	0.0081	0.0001	
	CV	<b>0.0230</b>	<b>0.0226</b>	0.0004	<b>0.0077</b>	<b>0.0076</b>	<b>0.0002</b>	<b>0.0064</b>	<b>0.0064</b>	<b>0.0000</b>	
ALE	XGB_OF	train	0.4473	0.0498	<b>0.3975</b>	0.1376	0.1135	<b>0.0240</b>	0.1109	0.0864	<b>0.0245</b>
		val	1.9073	*	2.3566	0.1270	*	0.1507	0.0656	*	0.1164
		CV	<b>0.3113</b>	*	0.4167	<b>0.0366</b>	0.0099	0.0267	<b>0.0323</b>	0.0071	0.0252
XGB_OT	train	0.0356	0.0302	<b>0.0054</b>	0.0177	0.0141	<b>0.0037</b>	0.0130	0.0112	<b>0.0017</b>	
	val	0.0752	<b>0.0186</b>	0.0565	0.0321	0.0096	0.0226	0.0189	0.0076	0.0113	
	CV	<b>0.0344</b>	0.0227	0.0116	<b>0.0108</b>	<b>0.0065</b>	0.0043	<b>0.0076</b>	<b>0.0053</b>	0.0024	

\* Due to instabilities in variance estimation for ALE, likely caused by unstable bin assignments, the estimated  $\text{Var}_{\text{Est}}$  sometimes exceeds the estimated  $\text{Var}_{\text{Tot}}$ . We omit  $\text{Var}_{\text{Mod}}$  in these cases.

Fig. 3: Mean estimation errors on *SimpleNormalCorrelated* for  $X_1$  and  $X_3$ . For each sample size  $n$ , variances are averaged over all grid points. Axes are log-scale.